agriculture

MDPI

Review

Leveraging on Advanced Remote Sensing- and Artificial Intelligence-Based Technologies to Manage Palm Oil Plantation for Current Global Scenario: A Review

Mohammad Nishat Akhtar [1], Emaad Ansari [1], Syed Sahal Nazli Alhady [2,*] and Elmi Abu Bakar [1,*]

[1] School of Aerospace Engineering, Universiti Sains Malaysia, Engineering Campus, Seberang Perai 14300, Malaysia
[2] School of Electrical and Electronic Engineering, Universiti Sains Malaysia, Seberang Perai 14300, Malaysia
* Correspondence: sahal@usm.my (S.S.N.A.); meelmi@usm.my (E.A.B.); Tel.: +60-19-6691441 (S.S.N.A.); +60-16-4939839 (E.A.B.)

Abstract: Advanced remote sensing technologies have undoubtedly revolutionized palm oil industry management by bringing business and environmental benefits on a single platform. It is evident from the ongoing trend that remote sensing using satellite and aerial data is able to provide precise and quick information for huge palm oil plantation areas using high-resolution image processing, which is also recognized by the certification agencies, i.e., the Roundtable on Sustainable Palm Oil (RSPO) and ISCC (International Sustainability and Carbon Certification). A substantial improvement in the palm oil industry could be attained by utilizing the latest Geo-information tools and technologies equipped with AI (Artificial Intelligence) algorithms and image processing, which could help to identify illegal deforestation, tree count, tree height, and the early detection of diseased leaves. This paper reviews some of the latest technologies equipped with remote sensing, AI, and image processing for managing the palm oil plantation. This manuscript also highlights how the distress in the current palm oil industry could be handled by mentioning some of the improvised monitoring systems for palm oil plantation that could in turn increase the yield of palm oil. It is evident from the proposed review that the accuracy of AI algorithms for palm oil detection depends on various factors such as the quality of the training data, the design of the neural network, and the type of detection task. In general, AI models have achieved high accuracy in detecting palm oil tree images, with some studies reporting accuracy levels up to 91%. However, it is important to note that accuracy can still be affected by factors such as variations in lighting conditions and image resolution. Nonetheless, with any AI model, the accuracy of algorithms for palm oil tree detection can be improved by collecting more diverse training data and fine-tuning the model.

Keywords: palm oil; remote sensing; artificial intelligence; tree count; tree height; health mapping; image processing; precision agriculture

Citation: Akhtar, M.N.; Ansari, E.; Alhady, S.S.N.; Abu Bakar, E. Leveraging on Advanced Remote Sensing- and Artificial Intelligence-Based Technologies to Manage Palm Oil Plantation for Current Global Scenario: A Review. *Agriculture* **2023**, *13*, 504. https://doi.org/10.3390/agriculture13020504

Academic Editors: Paul Kwan and Wensheng Wang

Received: 31 December 2022
Revised: 6 February 2023
Accepted: 8 February 2023
Published: 20 February 2023

1. Introduction

Oil palms are considered to be an essential economic crop. Despite their core usage in palm oil production, they are also utilized to generate numerous products, i.e., furniture, paper, plywood, etc. [1–3]. Essential information with respect to the geographical location of the palm tree plantation plays a key role. Firstly, it is important for anticipating palm oil yield, which is widely used in vegetable oil in most part of the world. Secondly, it also gives us important information pertaining to the growth situation of the palm tree, i.e., the age or the survival rate of the palm. In addition to this, it also helps in the improvisation of the development of irrigation processes and thus maximizes productivity [1]. Oil palms are mostly grown in Southeast Asia and Africa, and are considered highly productive, producing more vegetable oil per hectare compared to other oil crops [4]. Table 1 shows the highest palm oil production countries in the world. However, these days, the conversion

of tropical forests to palm oil plantations has also tarnished the environmental system, resulting in the loss of a huge number of plant and animal species.

Table 1. World palm oil production countries (2019) (Source: Our World in Data).

Country	Production (Tons)
Indonesia	42,869,429
Malaysia	19,858,367
Thailand	3,040,000
Colombia	1,527,549
Nigeria	1,220,000
Guatemala	880,000
Honduras	707,000
Papua New Guinea	578,000
Ecuador	420,000
Ghana	257,280

Due to rising demand for more economical vegetable oil along with bio-fuel, the task is to raise the output of oil while reducing the influence on the planet's forests and also the environment. Table 2 shows the list of countries that consume the highest palm oil. In the year 2016, the typical crude palm oil return was 3.21 tons per hectare, whereas the fresh fruit bunch (FFB) as well as return and oil extraction rate (OER) arrived at 15.91 tons/ha, which was 20.18% less compared to 2015 on account of the protracted El Nino climate states [4]. As a result of many factors that may have had an influence, the target hit comprises the aforementioned natural conditions along with the absence of problem mitigation efforts. Smallholders remain most hit, although some plantation businesses were able to deliver six tons per year. Therefore, it has become deemed necessary to come up with necessary steps that can increase the yield of the palm oil.

Table 2. Worldwide major consumers (Source: Our World in Data).

No.	Country	2005 (1000 Tons)	2012 (1000 Tons)	2013 (1000 Tons)	2016 (1000 Tons)	2019 (1000 Tons)
1	India	3309	7588	8352	10,250	9732
2	European Union	4368	5700	6515	6600	9101
3	China	4340	6090	6239	5150	7552
4	Pakistan	1546	2040	2138	3300	3165
5	Egypt	591	573	626	1600	1105
6	Bangladesh	442	846	1193	1500	1335
7	United states	376	947	1269	1250	1582
8	Myanmar	308	563	735	900	902
9	Russia	264	523	589	800	1061
10	Vietnam	198	475	516	780	842

Global palm yields have increased over time, whereby over the last 50 years, the amount of land devoted to growing palm oil has increased substantially. As per Figure 1, it can be observed that since 1980 the amount of land the world used to grow palm has more than quadrupled, from 4 million to 19 million hectares in 2018. In this regard, Indonesia and Malaysia account for 63% of global land use for palm. In this aspect, in order to assess the land use on a local scale the conventional method is pricey and time consuming [5]. As a feasible approach, remote sensing along with image segmentation can be thought to be a viable choice for oil palm monitoring involving the amount of oil palm output [6–8].

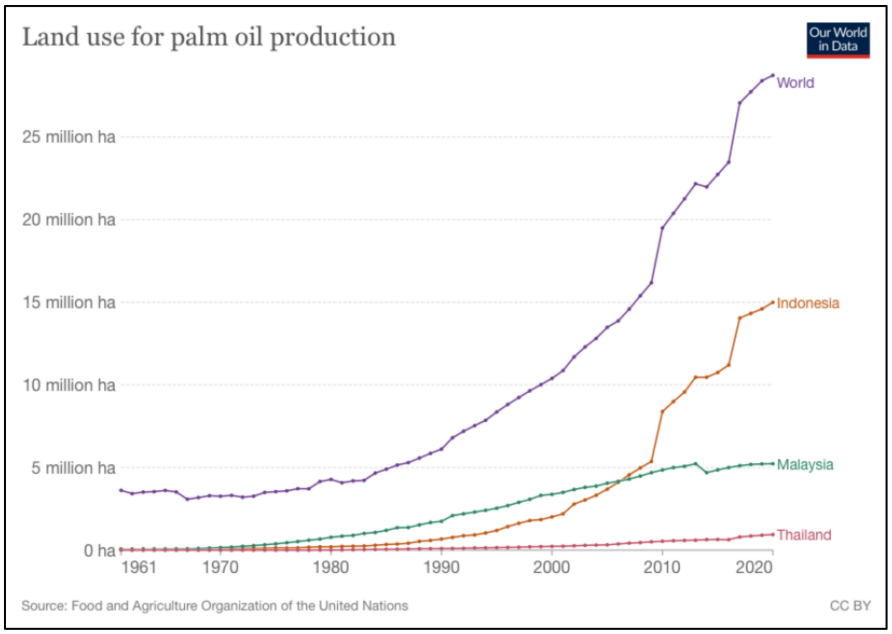

Figure 1. Change in land use for palm oil production (Source: Our World in Data).

So far, palm oil plantations have been tracked using time-consuming and costly evaluations, and lots of nations lack the tools to perform regular surveys. Remote sensing has become a possible alternative for determining oil palm locations, utilizing high performance satellite vision systems. In addition, it provides the necessary independent tracking required for certification agencies such as the Malaysian Palm Oil Board (MPOB), the Roundtable on Sustainable Palm Oil (RSPO), and the United Nations Framework Convention on Climate Change (UNFCC) [6]. Basically, these organizations ensure the goal that oil palms should be handled responsibly and should be sustainable in the environment, whereby remote sensing provides invaluable geographical information that is needed to monitor the conditions of oil palms at large area coverage. Therefore, spatial data have become more and more significant in this respect. Remote sensing accelerates multitudes of application data that can be interpreted into valuable information [9,10]. Whilst analyzing the capacity of remote sensing in oil palm cultivation, application-oriented research experiments can generate profit. These experiments need to find solutions for numerous dilemmas faced by the oil palm business, i.e., prohibited deforestation, the dispersing of pests or disease, nutrient deficit detection, yield estimation, palm tree count, and the observation of degradation-related problems pertaining to oil palms [11,12]. Remote-sensing functions are an efficient tool to present the observation and early detection of these issues.

The management of palm oil plantations has been a subject of critical analysis due to a range of environmental, social, and economic concerns. Some of the key issues include:

1. Deforestation: The large-scale conversion of forests to palm oil plantations has resulted in significant deforestation and the loss of biodiversity. This has raised concerns about the impacts on wildlife and ecosystem services, such as carbon sequestration and water regulation.
2. Human rights: There have been numerous reports of human rights abuses in palm oil production, including forced labor, child labor, and land grabs.
3. Environmental impacts: The use of chemicals and fertilizers in palm oil production can lead to water pollution and soil degradation, while the burning of forests to clear land for plantations can contribute to air pollution and climate change.
4. Sustainability: There is a growing demand for sustainably sourced palm oil but certifying palm oil as sustainable can be challenging due to conflicting interests and a lack of standardization in certification programs.

Despite these challenges, there have been efforts to improve the management of palm oil plantations and ensure that they are more sustainable and responsible. This has included initiatives to promote responsible sourcing, reduce deforestation, protect human rights, and minimize environmental impacts. Therefore, the management of palm oil plantations remains a complex and critical issue, with a range of challenges that need to be addressed. However, with continued efforts and commitment, it may be possible to achieve more sustainable and responsible palm oil production by leveraging Artificial Intelligence (AI) and advanced remote sensing.

The rest of the article is organized as follows: Section 2 starts with a compilation of remote sensing applications in numerous aspects of palm oil monitoring, followed closely by Section 3, which gives an AI perspective on palm oil planation management with regard to tree detection. Section 4 emphasizes remote sensing-based algorithmic solutions for palm tree health and height assessment, and Section 5 illustrates the role of image processing in disease assessment for palm trees using a case study. Section 6 highlights the approach toward the sustainable production of quality palm oil, and finally Section 7 presents the conclusions of the proposed review.

2. Remote Sensing Techniques for Palm Oil Plantation Management

This sections gives a detailed overview of some of the advanced remote sensing techniques applied until now in the fields of land cover mapping, tree count using convolutional neural networks, the determination of tree height and tree health mapping.

Land Cover Mapping

With the advent of change in land cover mapping, land use land cover (LULC) analysis has become essential. During the twentieth century, the world's population grew from over 1 billion to about 8 billion people today. At the same time, the concentration rate of the population in cities also steadily increased, due to which cities expanded. As per the 1960 census data, on average 34% of populations resided in cities, which became 54% in 2014, and finally, it is anticipated that the concentration of populations in cities will touch 60% by 2030 [13]. This global trend concerns emerging countries more than developed countries, because of the high degree of deforestation on the outskirts of cities. Malaysia can be taken as an example of dynamic land cover shift, where more than 90% of the nation's highlands were forested, and now the percentage of forest cover is just over 4%. This has also resulted in the cultivation of palm oil in marginal soils, which are known as peats (Table 3). As per the remote sensing survey conducted in Malaysia in 2003, it was revealed that 313,000 ha of palm oil was cultivated on marginal soils/peats [14]. Digital classification using object-oriented techniques or visual classification have always been a favorite approach for LULC classification. The enhanced digital image could be segmented using optimized K-Means learning algorithm and could be deployed on cloud machines for high-speed processing [15].

Table 3. Palm oil and palm trees on peat land areas (2016) (Source: MPOB).

Region	Total Palm Oil (ha)	Total Peatland (ha)	Palm Oil on Peatland (ha)	Percentage of Palm Oil on Peatland (%)
Peninsular Malaysia	2,714,254	891,700	546,480	61.3
Sarawak	1,506,769	1,449,440	866,110	59.7
Sabah	1,551,714	190,890	91,940	48.2
Total	5,772,737	2,532,030	1,504,530	59.4

In order to have a global understanding of urban ecosystems and their ever-changing plant biodiversity, remote sensing imagery offers greater observation capabilities and new perspectives compared to in situ experimental means. Indeed, remote sensing has the advantage of being able to study different spatial scales at several time periods, notably

thanks to airborne acquisitions at metric to decimetric resolutions, and thanks to the numerous satellite constellations offering a wide range of coverage to cities and towns [16]. Nevertheless, the use of remote sensing is constrained by the strong heterogeneity of the elements characterizing an urban scene [17]. Depending on the applications targeted, the instrumental characteristics (spatial and spectral resolution, noise) and the acquisition configurations (angular aim of the sensor, revisit time) are determining factors for a certain scale of observation [18].

Image acquisition using satellite sensors such as LANDSAT and ASTER, with a low spatial resolution and ground sample distance (GSD) greater than 10 m is sufficient to understand urban heat island phenomena at the agglomeration scale [6], the evolution of demographic extension [19] or the observation of air pollution [20]. However, these acquisitions are too unresolved for other applications based on a more detailed cartography of the pictorial scenes. In fact, under these conditions, only a small number of classes of surface elements can be discriminated, among which we can distinguish between occupied and unoccupied areas, and possibly urban forests. In terms of mapping accuracy, the recently phased array type-L band synthetic aperture radar (PALSAR) mounted on the advanced land-observing satellite (ALOS) was used for evaluation by Cheng et al. [21] and its comparison was performed with MPOB palm oil mapping. The PALSAR was implemented using maximum likelihood classification (MLC) for palm oil mapping. Table 4 shows the comparison of mapping between PALSAR and MPOB. It is evident from the table that the best accuracy attained using PALSAR palm oil mapping was 94.50% whereas the average palm oil mapping accuracy attained using PALSAR was 89.78%.

Table 4. Comparison between the best estimated oil palm area from PALSAR-2 and MPOB (Source: MPOB).

State	State Area (Mha)	Best Area (Mha)	MPOB Palm Oil Area (Mha)	Best Map			
				Resolution	Area Difference 1 (Mha)	Area Difference 2 (%)	Area Difference 3 (%)
Johor	1.921	0.868	0.739	25	0.129	17.46	6.72
Kedah	0.95	0.212	0.087	50	0.1250	143.68	13.16
Kelantan	1.510	0.140	0.151	100	−0.0110	−7.28	−0.76
Melaka	0.166	0.056	0.054	25	0.0020	3.7	1.20
Negeri Sembilan	0.669	0.1769	0.177	25	−0.0001	−0.06	−0.01
Pahang	3.614	0.711	0.725	100	−0.0140	−1.93	−0.39
Perak	2.104	0.56	0.398	100	0.1620	40.70	7.70
Perlis	0.82	0.003	0.002	25	0.0010	50	1.22
Pulau Pinang	0.105	0.013	0.014	25	−0.0010	−7.14	−0.95
Sabah	7.363	1.495	1.544	100	−0.0490	−3.17	−0.67
Sarawak	12.445	1.495	1.544	50	0.056	3.89	0.45
Selangor	0.810	0.140	0.137	25	0.003	2.19	0.37
Terengganu	1.304	0.207	0.172	100	0.0350	20.35	2.68
Total	33.043	6.135	5.639	100	0.4960	8.80	1.50

Nevertheless, the emergence of spatial instruments with spatial resolutions of less than 5 m, such as IKONOS, Quickbird, SPOT, WorldView, and recently Pleiades, also allow a better distinction of the variability of the surfaces encountered in urban environments, in spite of the increasing contribution of airborne imagery. In particular, Alonzo et al. [22] took an inventory of plant biodiversity in Santa Barbara, California through acquisitions with the AVIRIS sensor at a resolution of GSD = 3.7 m. Rosenbaum et al. [23] studied road traffic surveillance with aerial images at GSD = 0.2 m and with respect to multi-spectral classification. Roessner et al. [24] constructed a classification of 38 spectral identities of materials with the DAIS sensor on the city of Dresden in Germany.

Ultimately, there is no optimal spatial resolution for entire applications. However, the characterization of urban environments for classification requires GSD values close to 5 m [25] and the study of urban vegetation, for its part, requires a GSD of at least less than 0.5 m in order to distinguish crowns from trees [26]. However, as much as the visual reading of the image becomes easier with the increase in the spatial resolution, the spatial

analysis of the scene also becomes more complex, because on this scale the 3D dimensions of the objects and the topography of the ground are no more negligible [27]. Several characteristics specific to urban environments are to be taken into account to standardize the optimal spatial resolution pertaining to the specific application. Some are listed as: slope effects, shadowing effects, and undesirable shading effects caused by the presence of both buildings and trees.

It is widely recognized that land use/cover change (LULCC) on the local and global scales is one of the crucial driving factors of climate change [28]. The Intergovernmental Panel on Climate Change (IPCC) from 2007 reported that human actions, such as urbanization, were to great concern due to the countless consequent modifications that were created to the Earth's surface. Some researchers showed that human-induced LULCC including urbanization was among the vital elements that influenced regional urbanization, which is advantageous to the economic welfare of individuals and the whole of society but impacts towns' biophysical wellbeing. This phenomenon causes harm to environmental parameters such as biodiversity [29] and soil fertility [30], and has effects on other organic sources along with the ecosystem [17]. Among the most researched phenomena of land use is urban land transformation, which becomes irreparable due to land use shift [31]. Urban land use modifications, e.g., the loss of plants, enlarged foliage and open spaces, as well as the greater expanse of urban materials such as concrete and asphalt, may change the climatic conditions of any place through the modification of a number of physical and biological components of the ecosystem [32]. These involve vegetation, the presence of moisture, and impervious built-up cover, and soil properties, air and surface temperature, etc., which are affected in turn due to massive urbanization [33]. In Malaysia, Iskandar Malaysia (IM) is considered as one of the fastest economic growth areas. It is considered that the region will be changed into a great metropolis from 2025 with an approximate 3 million population [7].

The transformation of the metropolitan land-use pattern of Malaysia continues to have an increasing trend. With that aspect, traditional mapping and studying approaches are costly in terms of time and money. Therefore, it is deemed necessary to come up with a technique to comprehend urban land use patterns via image processing. In the past couple of decades, mainstream research recognizing urban land use patterns has been based on high spatial resolution (HSR) image stream classification [18]. High spatial resolution graphics possess an important component of geospatial statistics, and can be broadly used to extract urban land use info. The extracted data classify land cover type by characteristics, such as scope, texture, and the form of various property parcels [25]. Urban land use patterns have been closely correlated with resident pursuits and government rules. The inner design of metropolitan land usage is complicated where the alleged 'semantic gap' requires dedicated analysis. To put it differently, comprehending conditions necessitates the consideration of this arrangement and the makeup of ground objects. This sort of consideration takes a significant personal effort to obtain high-level semantic advice and then to categorize precisely the urban land use form through sophisticated remote sensing-based image processing domains. The state of the art of improving urban land use via such sophisticated systems was represented by Vu et al. [34], who implemented a probabilistic theme version (PTM) to fuse spectral and textural features from HSR images. However, in their work most remote sensing procedures are employed on property parcels with contours. When the qualities of the images are all expressed, an irregular parcel trigger is generated. Exclusively, with a growth in image spatial resolution, the spatial arrangement of the Earth's surface components shows a recognizable heterogeneity, which ends at a multi-scale effect confusion as to whether these features are categorized or not. This confusion represents a great difficulty when faced with object-oriented classification procedures. A small number of scientific reports have focused on image information with networking information to classify urban property use adopted using Landsat remote sensing pictures and point of interest (POI) information to determine urban land use specifications. Liu et al. [35] applied Worldview-2 graphics and tons of social network data sources with PTM to detect the metropolitan land use condition in Guangzhou (China)

and achieved comparatively impressive outcomes. Probing deeper into HSR graphics to get high speed accurate info to interpret the metropolitan spatial transformation is now a favorite new research topic. Huang et al. [36] exploited a deep-learning method and created HSR image sub-sets to deal with multi-scale image analysis in remote-sensing data classification. Nowadays, with regard to numerous areas of research, it has become evident that Artificial Intelligence is successful in resolving the 'semantic gap' issue in dystopian classification as it averts launching a complicated, rule-based classifier. Profound understanding warrants further investigation and reflects a very promising strategy with Artificial Intelligence analysis that could be applied in various countries.

3. Role of Artificial Intelligence in Palm Tree Identification

Artificial Intelligence (AI)-based methods have become essential and are very widely used for the majority of applications pertaining to palm tree identification. Palm tree or shrub crown discovery studies have been predicated on methods using AI. To take a single instance of these, a shrub discovery-delineation algorithm was first implemented for tree elevation detection, which was based upon the neighborhood likely filter to determine the tree apex [37]. Chen et al. [38] introduced a method for oil-palm detection on the basis of a tree elimination technique, which works on the principle of high spatial resolution airborne imagery statistics made up of numerous components, i.e., empirical investigation, texture analysis, boundary augmentation, segmentation treatment, morphological identification, and blob examination. Upgupta et al. [39] applied semi-variogram computation and also non-maximal suppression for palm tree manipulation out of top-heeled multi-spectral satellite graphics. Lakshmi et al. [40] utilized a scale-invariant feature transform (SIFT) with machine learning to find palm oil trees using unmanned aerial vehicle (UAV) images. Plowright et al. [41] utilized the circular autocorrelation of polar silhouette matrix representation of the image using the shape characteristic method to emphasize the identification of the selected attribute of the palm tree.

The identification of densely arranged palm trees has gained more attention in terms of research perspectives. Srestasathiern et al. [42] came up with a novel method to identify the crown of palm trees with a high precision rate. With the help of semi-variogram-based AI model analysis, they were able to detect window size without any manual modification. On the contrary, their approach was only confined for spatially arranged palm trees whose crowns did not overlap with each other. Shaharum et al. [43] came up with a novel approach in which they utilized high spatial resolution image data, inclusive of multiple components comprising image segmentation, image morphology, spectral and textural analysis, etc. However, even their method was not suitable to be applied on densely populated palm trees. The research from the past couple of years depicts that deep learning-based systems additionally have already been utilized for hyper-spectral image classification [44], large scale land classification [45], spectacle type [17], and also object discovery [46], etc., using the remote sensing domain and attained much greater performance than conventional methods. For example, Cheang et al. [47] introduced the idea of profound comprehension and utilized the stacked auto-encoder approach into hyper-spectral remote sensing image classification. Moreover, Nogueira et al. [48] evaluated the strategy to exploit the famous existing deep convolutional networks-based AI model (ConvNets) for remote sensing applications using fine tuning descriptors with a linear SVM classifier. In their evaluation, the pre-training of the feature extractors was performed using the ImageNet and Places205 [49] datasets. Table 5 shows the accuracy of the assessed models implemented on Brazilian coffee fields by Nogueira et al. [48]. Nonetheless, their research opens up a new paradigm for an enhanced spectral spatial feature representation.

Table 5. Accuracy of the assessed models on Brazilian coffee fields.

Models	Accuracy
$Overfeat_L$ [50]	90.91%
$Overfeat_S$ [50]	90.13%
AlexNet [51]	93%
CaffeNet [52]	93%
GoogleNet [53]	92.80%
$Overfeat_L$ [50]	90.91%

State-of-the-art research for automated palm tree detection using deep learning-based AI methods was carried out by Li et al. [37]. They used the convolutional neural network (CNN) to identify palm trees accurately for both spatially well-arranged as well as densely populated patterns. Moreover, Li et al. [37] also evaluated their proposed algorithm with an artificial neural network (ANN), local maximum filter and template matching algorithm. It is worth noting that local maximum filter and template matching algorithms are considered to be the traditional methodologies for crown detection. Li et al. [37] implemented and assessed their proposed algorithm using the aforementioned techniques on three different regions, i.e., R1, R2, and R3 with different distributions and patterns of palm oil trees. Table 6 shows the accuracy for four different algorithms implemented on R1, R2, and R3 to detect the number of palm trees.

Table 6. Accuracy of different algorithms to detect count of palm trees.

Techniques	R1	R2	R3
Convolutional Neural Network	1651	1607	1683
Artificial Neural Network	1648	1585	1679
Template Matching Algorithm	1429	1392	1608
Local Maximum Filter	1493	1397	1643

The chief parameters of the CNN are considered to be the selection of kernels from the very first convolutional layer, the range of all kernels from the second convolutional layer, and also the number of concealed units from the fully connected layer.

The following sub-sections discuss all of the parameters used in the CNN-based AI model that was implemented by Li et al. [37]. Based on their proposed method, more than 96% of the oil palm trees in their study area could be detected accurately.

3.1. CNN Training and Parameter Optimization

The LeNet neural system is constructed of two convolutional layers and two pool layers along with a completely connected layer, as shown in Figure 2. The input to the fully joined/connected layer is the collection of all feature maps in the layer below. The fully connected layers correspond with a multilayer perception constructed by a logistic regression layer. Rectified Linear Unit (ReLU) is used as an activation part of this CNN. Within this study, Li et al. [37] interpreted 5000 palm tree samples along with 4000 background samples from their study area. A total of 7200 samples were picked randomly from the total samples as the training dataset of the convolutional system, and the other 1800 samples were taken as a dataset for evaluation purposes. The labelling for "palm tree" was performed only by determining its center in every sample. Each sample corresponded to 17 × 17 pixels comprising three rings (Red, Green, and Blue) chosen from the initial four bands. Until the ideal combination of parameters for which the accuracy is the maximum from 1800 test samples is determined, the CNN's parameters are corrected continuously. After parameter tuning, the finest version is achieved, which is supposed to be utilized in the process of label prediction for numerous image datasets.

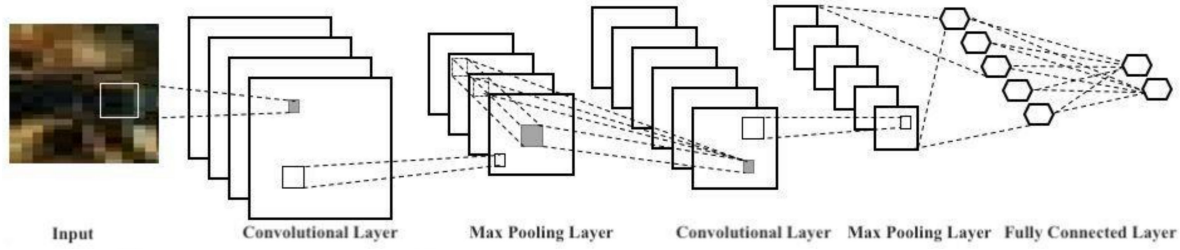

Figure 2. LeNet neural network of the palm oil tree image.

The training of a Convolutional Neural Network (CNN) for palm oil tree detection involved several steps, including data preparation, network design, loss function selection, and parameter optimization. The steps involved in CNN training and parameter optimization are summarized as:

1. Data preparation: The first step in training a CNN for palm oil tree detection is to prepare a large dataset of labeled images that are representative of the target application. This dataset is to be used to train the CNN and to evaluate its performance.
2. Network design: The next step is to design the CNN architecture. This involves selecting the number and type of layers, the size and type of filters, and the activation functions. The design of the CNN is to be optimized for the specific task of palm oil tree detection.
3. Loss function selection: The loss function is a measure of the error between the predicted output and the actual output. The loss function is used to guide the optimization of the network parameters. Common loss functions used for image classification tasks include cross-entropy loss and mean squared error.
4. Parameter optimization: During network training, the parameters of the network are optimized to minimize the loss function. This is typically done using an optimization algorithm, such as stochastic gradient descent, which adjusts the parameters based on the gradient of the loss function.
5. Back-propagation: The back-propagation process is to be used to compute the gradient of the loss function with respect to the network parameters. This gradient is then used to update the parameters in the direction that minimizes the loss function.

It is significant to note that training a CNN for palm oil tree detection involves a series of steps, including data preparation, network design, loss function selection, and parameter optimization. The back-propagation process is used to compute the gradient of the loss function and to update the network parameters. The goal of this process is to minimize the loss function and to achieve the best performance for palm oil tree detection.

3.2. Label Prediction

The image dataset for label prediction is gathered using the sliding window technique, as represented in Figure 3. The window's dimensions set by Li et al. [37] were 17 × 17 pixels, which was in accordance with the characteristic size of test samples and the training sample. However, this window size could be changed as per the spatial distribution of the palm tree. Using this sliding window, the count of the palm trees is detected. In case the sliding step is too big, then the palm samples will not be detected and will be missed. If the sliding step is too small, then the repeated detection of one palm tree sample becomes possible. The process of label prediction tends to become slower because if the quantity of samples in the image dataset increases, then it results as least importance with waste of time. Through evaluations, the sliding step is defined as three pixels in the analysis performed by the author W. Li et al. [37]. Post-collection of all the samples of the image dataset through the sliding window procedure, the best CNN model is selected for every sample from the image dataset.

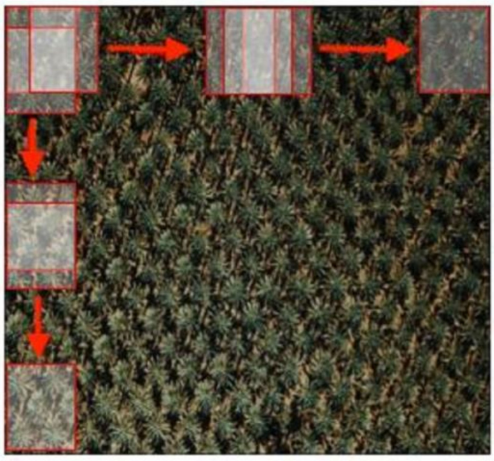

Figure 3. Label prediction using sliding window technique (Red squares represent sliding window).

3.3. Sample Merging

Post-label prediction of the image sample, the spatial coordinates for all the input image samples were gathered to determine the samples that were predicted as the class of "palm tree". Now, the coordinates for the number of predicted palm tree classes could correspond to several palm trees in reality, i.e., one palm tree's coordinate could correspond to three palm trees in the original input sample. In order to overcome this problem, the coordinates corresponding to the palm tree sample were merged into a single coordinate iteratively, as shown in Figure 4. Assuming that, in the study region, the distance between two palm trees cannot be less than eight pixels, its corresponding merging would require six iterations. For each iteration, every coordinate group using the Euclidean distance under a specific threshold is supposed to be merged into a single coordinate [37].

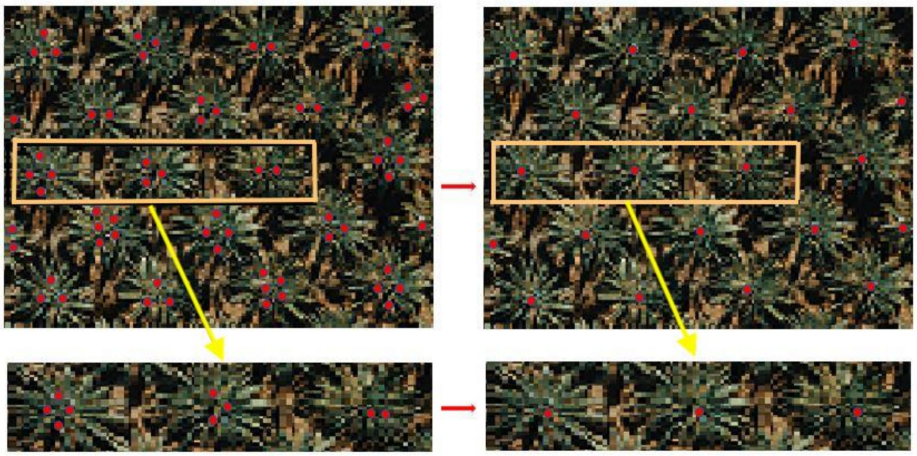

Figure 4. Estimation of tree count using sample merging technique.

In palm oil tree detection, a Convolutional Neural Network (CNN) is often trained using a specific type of loss function known as a binary cross-entropy loss. This loss function is appropriate for image classification tasks where the goal is to predict the presence or absence of an object, such as a palm oil tree, in an image.

The binary cross-entropy loss function is defined as in Equation (1):

$$L = -(y \times \log(p) + (1 - y) \times \log(1 - p)) \quad (1)$$

where y is the true label (0 or 1), p is the predicted probability of the positive class (i.e., the probability that a palm oil tree is present), and log is the natural logarithm. The binary cross-entropy loss function is used to evaluate the difference between the predicted probability

and the true label, and the goal is to minimize this difference. During the training process, the parameters of the CNN are adjusted so as to minimize the binary cross-entropy loss.

It is worth noting that the binary cross-entropy loss function is a commonly used loss function for training a CNN for palm oil tree detection, as it is appropriate for image classification tasks where the goal is to predict the presence or absence of an object. The goal of using this loss function is to minimize the difference between the predicted probability and the true label, and to achieve the best performance for palm oil tree detection.

4. Assessment of Palm Tree Health Mapping and Height

The function of remote sensing approaches to evaluate and measure the effects of radicals has improved [54,55]. Standard approaches include the usage of image and spectral detectors through manned satellite and aircraft technologies [56]. These are used for the calculation of indicators [56,57] and regression units in the server array [58,59]. Nonetheless, these processes are primarily concentrated on quantification and distribution, along with other physiological properties of wood species. Satellite and unmanned aircraft studies have reported limits regarding resolution, operational expenditures, and unfavorable climate conditions (e.g., cloudiness and danger storms) [31]. By comparison, the constant evolution of unmanned aerial vehicle (UAVs) layouts, navigation systems, mobile image detectors and cutting-edge system learning procedures allow discreet, precise, and flexible surveillance tools for precision farming and bio-security [60]. Studies have put UAVs for airborne imagery in an assortment in domains, i.e., for weed or marijuana growth detection and wildlife observation [31,60].

A greater NDVI value suggests a healthy tree. Clearly, the leaf size, leaf water content, leaf pigmentation, and the stem arrangement strongly influence these indices [61]. The NDVI works well in areas where vegetation species are homogeneous. Tree health mapping becomes complex in forests, where plant species have varied histories and are more heterogeneous [62]. For instance, a heighted and healthier conifer tree might have the same NDVI value as an unhealthy deciduous tree [63]. To fix this difficulty, a multiple masking algorithm was used to perform the tree health mapping for every physiognomic tree type [64]. The initial mask was created based on the land cover type. This mask was utilized to mask all non-vegetation. The rest of the vegetation was merged into five layers depending on the physiognomic tree kind [65]. These layers comprised broadleaf deciduous conifer, palm, and mixed. Clustered and shrub trees were included by the mixed layer [66]. The trees that were clustered were defined as numerous trees that had crowns. Initially, health analysis was carried out on a low scale. A pixel-based analysis of the NDVI value and shrub health from the field survey was conducted for every type of tree. The thresholds for both wellness and NDVI indicator were decided based on histogram evaluation for both healthy and unhealthy trees at the sample [65]. The pixels for every tree crown were classified as healthy or unhealthy. The NDVI threshold was set as 31 to get a broadleaf deciduous tree, 30 to get a broadleaf evergreen tree, and 24 for both palm and conifer trees. The NDVI values over the threshold were categorized as wholesome healthy pixel values, and the rest were categorized as unhealthy pixel values. The number of unhealthy and healthy pixel values, along with NDVI, were derived from every tree [62].

As depicted in Figure 5, several studies conducted by both government and non-government research associations demonstrate that a significant quantity of palm trees have been aging or are on the verge of aging, and thus there are greater chances that oil palm production is very likely to reduce if adequate measures are not taken to replant these aging trees in a timely manner [29]. Oil palm trees in turn have the potential to generate high quantities of FFB [67]. With a life of over 30 decades, palm trees will be likely to provide a significant return if cultivated in a timely manner. The peak yielding interval for a palm tree is during the age of 9–18; in the subsequent period, generating capacity gradually diminishes [29]. It is projected that by 2024, more than 30 percent of Malaysian palm trees will cross their peak yielding age, which in turn will drastically affect the Malaysian palm oil industry [68]. Government reports suggest that roughly half of the nation's palm trees

over 365,000 hectares are currently 26–38 years old, roughly 8 percent of the entire harvest region, whereas a further 126,000 hectares have trees spanning the optimum yield period. Trees that are not suitable because of these harvest statistics signify an inevitable decrease in production in the future. A long-term plan is deemed necessary as a means to replace aged trees employing fresh high-yielding varieties (HYV) on a constant basis [30,69]. Such long-term plans would be able to fulfil the lack of high-yielding palm oil trees. However, a delay in implementing such a program could be fatal to the palm oil industries. It is also worth noting that the Malaysian authorities invested USD 135 million for a nationwide palm oil tree replanting program in 2013 that also targeted small-scale industries [69]. Some research related to the health monitoring of palm oil trees was carried out by researchers. In this regard, Yarak et al. [70] explored the use of deep learning and aerial imagery for assessing palm oil tree health. The authors proposed a convolutional neural network (CNN) model to classify palm oil trees into healthy and unhealthy categories based on aerial imagery. The results showed that the proposed model could accurately classify palm oil tree health and had the potential to be used for large-scale palm oil tree health monitoring.

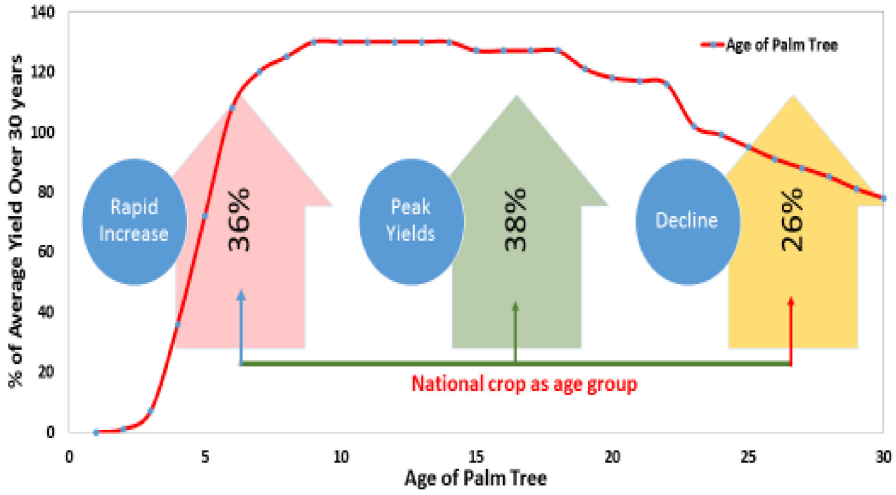

Figure 5. Ageing of palm oil trees.

Nonetheless, in the similar domain, Wibowo et al. [71] presented various methods of You Only Look Once (YOLO) variants for monitoring the palm oil tree and its health using UAV-based imagery and machine learning. Their results showed that their method was sufficiently accurate and efficient in detecting oil palm trees and had the potential to be implemented in commercial applications for plantation companies. With respect to the neural network paradigm, Ong et al. [72] proposed a method for improving palm oil tree health monitoring using deep learning and UAV imagery. They used a convolutional neural network (CNN) using the combination of AlexNet and SVM to classify palm oil trees into healthy and unhealthy categories based on UAV imagery. Their comparative studies showed that the overall performance of the AlexNet CNN model outperformed the AlexNet-SVM-based classifier.

In summary, the aforementioned reference papers investigated the use of aerial imagery and machine learning techniques for monitoring and assessing palm oil tree health and height. They showed that these techniques have the potential to be used for large-scale monitoring and management purposes, and they provide valuable insights into the potential of these techniques for improving palm oil tree health monitoring.

Determination of Tree Height

Global-scale carbon balance is the key to climate-change. Forests are considered to be large bronchial carbon sinks, and large proportions of carbon have been deposited in forests as biomass [73]. Tree above ground biomass (AGB) is the entire sum of organic matter living above ground within trees, such as leaves, twigs and branches, main bole and

bark [74]. Estimates of forest AGB have a significant role in estimating carbon stocks. The harvest of trees provides exact AGB estimates, but this process is time and labor intensive and also unrealistic on an average basis. With the help of shrub allometric relationships among tree features (AGB, stem diameter, tree height, crown size, etc.), field biomass is usually anticipated via the construction and application of allometric models that can be developed with AGB dimensions and shrub atomic variables [75,76]. Tree diameter at breast height (DBH) is believed to be an important factor in imitating tree above ground biomass. Consequently, DBH-based equations have been created for AGB at global scales [74,77]. Yet, despite using allometric models, it is infeasible to quantify each single tree from a large spatial scale. Remote sensing devices enable quotes at large-scale, beating the problems of ground sampling [78]. Previous studies have demonstrated that LiDAR is a reliable way to quote AGB, because LiDAR is able to accurately evaluate essential features (basal area, canopy elevation, shrub density, along with stem level, crown diameter, etc.) [79,80].

It is also worth noting that these wood structural traits are generally highly connected with AGB. The LiDAR systems tend to estimate AGB at the rack level, including aerial Wave Type LiDAR [81,82], aerial different -Yield LiDAR [41,83]. Regression analyses between field AGB anticipated with conventional allometric approaches and LiDAR duplex elevation indices have become the most usual means to come up with the LiDAR-AGB models.

Advanced airborne system-based LiDAR is integrated with a remote sensing system [12,84] for statistical modelling strategies [85–87]. Contemplating that AGB has been projected through allometric methods with respective tree measurements (e.g., DBH and height) as inputs, it could be anticipated that allometric methods will have substantial affects using LiDAR-based AGB model prediction [74,88].

It is an important aspect to understand underlying mechanisms that hinder the progress of this LiDAR-AGB version, as it plays an essential role in determining error for the LiDAR-based AGB model [4,89]. However, with LiDAR-AGB models it remains poorly understood up to what extent tree height-DBH provides allometric version residuals [74]. The enormous variance of all height-DBH version residuals would challenge LiDAR's capability of estimating field AGB, as long as it increases the issue of duplex vertical factors that influences DBH-based AGB quotes [90]. Adding tree height in field AGB estimates is supposed to reduce the consequences of the height-DBH model. Residuals pertaining to LiDAR model performance are due to the inclusion of AGB variation at specified shrub elevation. Incorporating both DBH and elevation as inputs in field AGB quotes enriches the association between field AGB quotes and LiDAR canopy metrics [91].

A digital elevation model (DEM) or even a digital terrain model (DTM) can be utilized for bare ground modelling without considering the characteristics on the ground surface [92,93]. On the other hand, digital surface models (DSMs) take into consideration the features on the Earth's surface, e.g., buildings and trees [94,95]. Methods utilized to create photogrammetric methods are usually focused on by DSMs. However, this technique needs well-functioning state-of-the-art cameras. Some examples of this retrieval of canopy height using multi-angle/multi-view passive vision from aerial platforms exist [96]. Emerging techniques of computer vision in improvised unmanned aerial systems (UASs) empower the extraction of dependable 2D along with 3D imagery information from the selection of multi-angle vision investigation taken with standard (non-metric) cameras and originated by Structure from Motion (SfM) algorithms [97,98].

Panagiotidis et al. [99] made a validation for determining tree height using UAV and ground measurement on two different plots, i.e., plot 1 and plot 2. Their workflow comprised a canopy height model (CHM) for tree height extraction, local maxima determination using raster image smoothening, and the implementation of inverse watershed segmentation (IWS) for crown diameter estimation. Their results are in agreement between the field and remote-sensed data for which the RMSE % was between 11.42 and 12.62 for height and 14.29 and 18.56 for the diameter of the crown. The statistical summary of the height estimates and the crown diameter estimates is shown in Tables 7 and 8 [99].

Table 7. Statistics of the measured and estimated crown diameter variables for the two study sites at the tree level.

Study Sites	RMSE (m)	RMSE (%)	Bias	Bias (%)	MAE (m)	P(T ≤ t) Two-Tail *t*-Test	t Critical Two-Tail *t*-Test	t-Stat	*p*-Value	df
Plot 1	3.00	12.62	−1.55	−6.99	2.62	0.15	2.01	4.14	0.00	47
Plot 2	3.08	11.42	2.35	8.02	2.88	0.00	2.02	7.27	0.00	38

Table 8. Statistical summary of crown diameter estimates for Plots 1 and 2.

Study Sites	RMSE (m)	RMSE (%)	Bias	Bias (%)	MAE (m)	P(T ≤ t) Two-Tail *t*-Test	t Critical Two-Tail *t*-Test	t-Stat	*p*-Value	df
Plot 1	0.82	14.29	0.43	6.92	0.73	0.00	2.01	4.17	0.00	47
Plot 2	1.04	18.56	0.70	11.11	0.80	0.00	2.02	5.61	0.00	38

It is worth noting that canopy height identifies the distance of the canopy top above the ground level. In order to determine the canopy height, the bare earth surface associated to the digital elevation model (DEM) is subtracted from the first return surface associated with the digital surface model (DSM) as shown in Figure 6. Both LiDAR area-based approach metrics, i.e., the top of the canopy height as well as the top of the canopy cover, are correlated with tree density and average plot associated to the tree height as shown in Figure 7 [37]. As per the experiment conducted by Li et al. [37], the height of the canopy cover was chosen as 3 m post comparison of unique models inclusive of height ranging between 1 and 23 m, to include a few different trees other than oil palm trees within the 1 ha plots. It can be clearly observed from Figure 7 that the influence of height is more on the top of the canopy; however, canopy cover at 3 m was heavily influenced by the density of the tree.

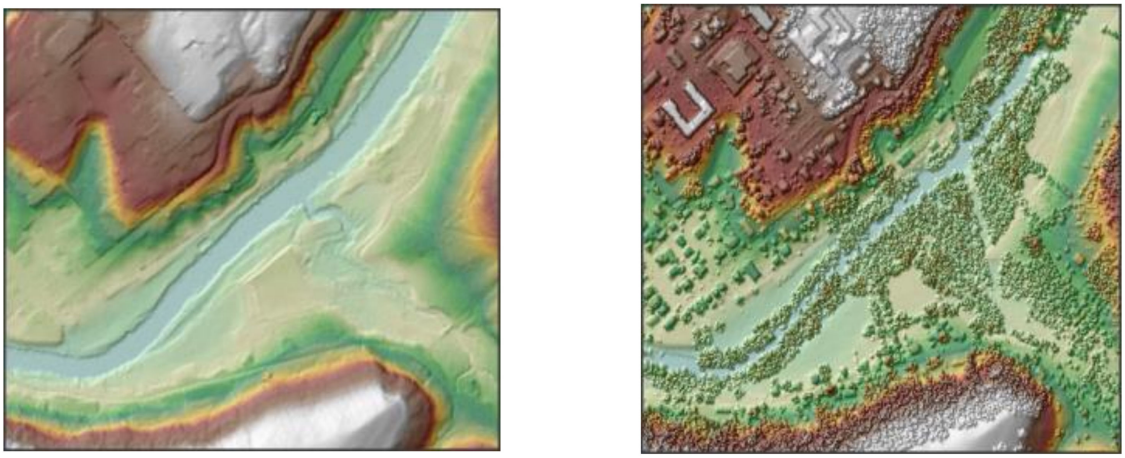

(**a**) (**b**)

Figure 6. Representation of Digital Elevation Mode (DEM) and Digital Surface Model (DSM); (**a**) DEM; (**b**) DSM.

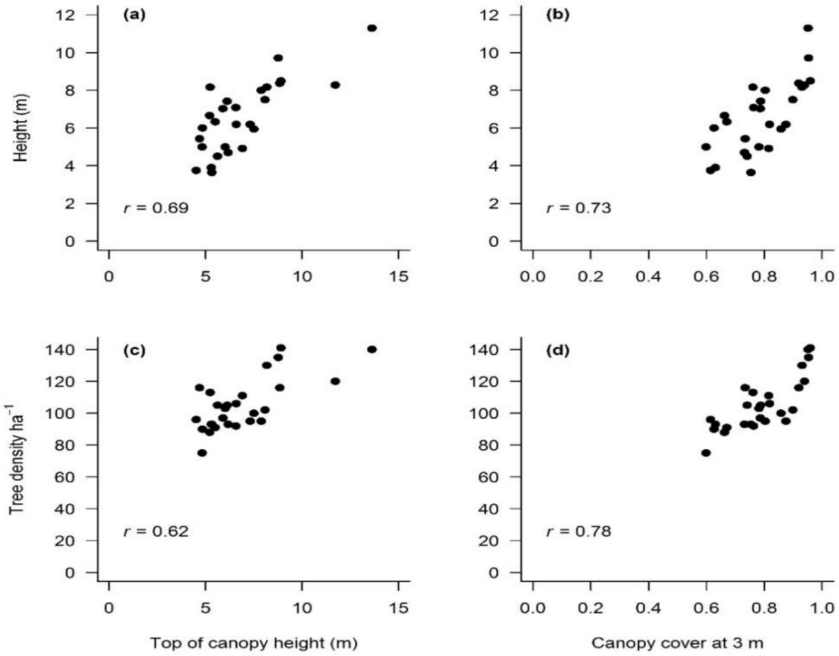

Figure 7. Correlation between top of canopy height with tree density and canopy cover with height [37].

5. Role of Image Processing in Disease Assessment

Leaf spots, leaf scorch, and leaf blight with tattering are all examples of bacterial diseases that commonly affect plants. There are two types of bacterial leaf spot diseases: those caused by fungi, which primarily affect stone fruit trees, and those caused by bacteria, which primarily affect vegetables such as tomatoes, peppers, and lettuce [100]. The symptoms and outcomes of both types of leaf spotting are comparable. Infected plants typically have uniformly sized brown or black water-soaked spots on the foliage, sometimes surrounded by a yellow halo. The browning of plant tissues, including leaf margins and tips, and the yellowing or darkening of veins are characteristic of leaf scorch (also known as leaf burn, leaf wilt, and sun scorch) [101]. This damage can cause the leaf to wilt and fall off. Leaves, branches, twigs, and floral organs quickly and completely chlorose, brown, and die due to blight. Many diseases that primarily manifest this symptom are therefore known as blights [102,103]. Many different pathogens can damage oil palm trees, just as they can damage most other crops. Fungal infections are the most common, and they stunt growth and reduce harvests [104,105]. Many countries that produce oil palms have reported several diseases in the trees. The most devastating oil palm disease in Indonesia and Malaysia is called basal stem rot or Ganoderma butt rot and is caused by the fungus Ganodermaboninense [106]. Sumatra suffers from severe aluminum deficiency in its oil palms [107,108]. There are more than forty diseases that can affect oil palms, and Smith et al. [109] documented them all. Germination (with brownish germ ailments), the toddler stage, and the discipline planting phase were all used to pinpoint the causes of the diseases. Deficiencies in potassium, phosphorus, boron, and calcium are likely to blame for the widespread seed decay and brown germ caused by S. commune in Malaysia [108,110–112].

First, the input leaf image in Red-Green-Blue (RGB) colorspace is converted to Hue-Saturation-Intensity (HSI) colorspace, as described by Singh and Misra [113]. This step is considered as the initial step in the image segmentation of a diseased leaf. In the second step, by using the threshold value, green pixels are masked and removed. For the third step, by using the pre-computed threshold level, the removal of green pixels and masking are performed for the useful segments that are extracted first in this step, prior to image segmentation. Lastly, in the fourth step, the segmentation is performed.

Image processing and a genetic algorithm implemented in Adruino were used by Arya et al. [114] to identify diseased leaves in plants. Histogram matching was used to identify the leaf's edge when it was diseased. Automated dead zone detection in 2D leaf images was used by Sahoo et al. [115]. Their research revealed that these threshold techniques were used to successfully lesion region area and to segment leaf area. Finally, the ratio between leaf area and lesion area is calculated to classify the disease. The results from the studies indicate that the proposed method is both efficient and accurate for estimating the degree of leaf disease and determining the leaf area. A leaf spot detection algorithm was developed by Bai et al. [116] and Ma et al. [93] and implemented with the help of neighborhood grayscale information. Diseased area detection was performed in their respective papers by contrasting the impact of the HSI, CIELAB, and YCbCr color spaces. Their work made use of Gaussian blur to filter the image. Finally, they calculated a threshold based on the color component of the leaf and applied Otsu's threshold method to identify the diseased area.

Numerous image segmentation algorithms have been used to study images over the years. Texture is an essential feature that reflects important information about the image surface and is used in a variety of algorithms for carrying out the process of image segmentation. The goal of image segmentation is to divide an image into distinct areas that represent distinct objects, surfaces, or an object's natural composition. Occlusion boundary estimation, image compression, visual database searching, and object recognition rely heavily on the segmentation process. Researchers today face the challenge of dealing with the oversegmentation of images, which leads to inaccurate results and, consequently, leaves room for improvement [117,118]. Image segmentation primarily deals with the degree of dissimilarity and degree of similarity between two images. Similarity corresponds to the process of combining and matching the pixels with the neighboring one based on its grey level pixel value match [119,120]. Dissimilarity is caused by sudden changes in the intensity of the image. Otsu's threshold method for automated image segmentation, region growing and region merging technique, edge detection method, watershed transformation, and histogram thresholding-based algorithms are just a few of the well-known methods used to implement image segmentation [121].

Otsu's method is the most well-known technique for performing image segmentation [122]. Considering it is a machine-driven procedure, it can readily be applied to large amounts of image data all at once. Since the proposed study involves working with images, the Open Computer Vision (OpenCV) library is a natural fit, and it should be noted that Otsu's threshold technique is highly compatible with OpenCV [123]. In addition, OpenCV is equipped to take advantage of a high level of parallelism using its extensive library [124]. With these parameters, efficient parallel image processing becomes a realistic possibility. Hadoop Map-Reduce is the only supported parallel programming model for the Hadoop Interface for Image Processing (HIPI), which is a comprehensive set image processing framework [125]. The Map-Reduce algorithm, which can be implemented on a cluster of nodes, has the capability to fully utilize HIPI's potential for high throughput image processing.

5.1. Analysis of Leaf Blight in Palm Leaf-Case Study

As per the initial experimental formulation carried out by Akhtar et al. [126], sample images from palm oil plantations were acquired from Universiti Sains Malaysia (47N 644134.94248273 591966.09761409) during the end quarter of the year 2019. As the initial images acquired had noise components, a bilateral filter was applied to remove the noise. After eliminating background noise, an HSV color space conversion of the blurred, transformed RGB image was performed to examine the affected areas of the plant's leaves. Once the different regions were analyzed, image thresholding was applied to isolate the infected areas. After the estimated diseased area was outlined, the contour was drawn to ensure precision. It is worth noting that leaf tattering can impact the health of the palm leaf, as shown in Figure 8a. The image has a resolution of 4000 $\times$ 3000 and was captured from 1 m away.

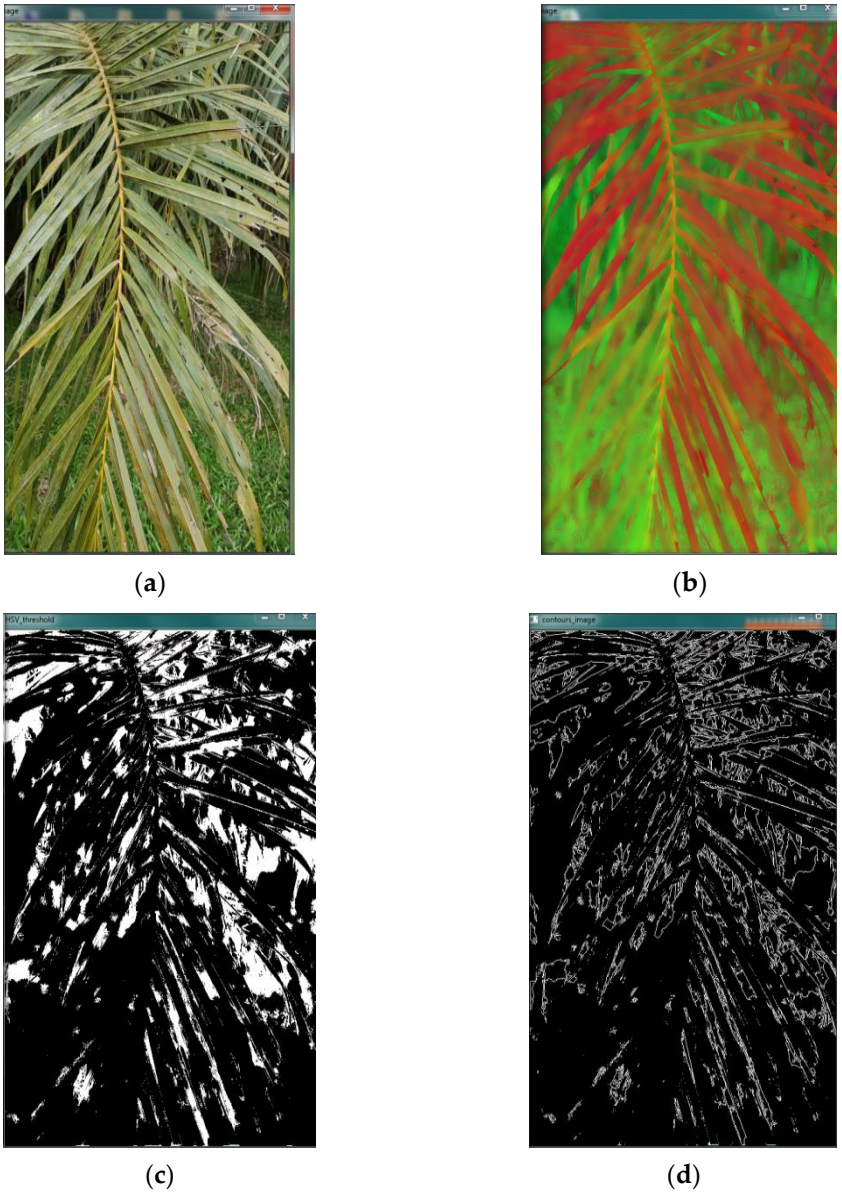

Figure 8. Analysis of leaf blight and tattering in palm tree (original resolution: 4032 × 3024) (**a**) Original image (**b**) Bilateral blur-based segmented HSV Image (**c**) Thresholding of segmented image (**d**) Defining contours.

Hue-Saturation-Value (HSV) is a useful color space for analyzing palm leaf tattering samples because it can be used to separate color components and adjust the intensity. It is important to note that each type of diseased leaf has its own distinct color palette. Following HSV threshold analysis, the total number of non-zero pixels could be used to determine the size of the affected region. Algorithm 1 shows the pseudocode for segmenting images.

Algorithm 1. *Requirements: Bundled input images*

1. Input image JPG format
2. Resize the image to 500 × 500//resize(img, image, size)
3. Apply filter (Bilateral Blur)//Bilateral Filter(image, dst,15,80,80)
4. Convert RGB colorspace to HSV colorspace//cvtColor(dst, HSV, CV_BGR2HSV)
5. Apply Threshold adjustments by adjusting the HSV trackbars
6. SegmentThresholded pixels//(0[Black],255[White] Pixels)
7. Draw contours
8. Store segmented pixels//white/black pixels
9. Emit segmented pixels variable//write(new IntWritable(1),newIntWritable (ROI pixels));

Table 9 shows the accuracy detection for leaf tattering in 20 test samples using three different color spaces on the thresholded image.

Table 9. Accuracy detection using different color spaces.

Diseased Samples	No. Of Images (Train Data)	No. Of Images (Test Data)	Detection Accuracy of Proposed Algorithm Using Different Colorspace (%)		
			HSV	CIELAB	YCbCr
Palm	25	20	100% (count of non-zero pixel: 58,485)	91%(count of non-zero pixel: 53,221)	90% (count of non-zero pixel: 52,636)

The detection accuracy on both the training and testing sets of diseased palm leaves is shown. Compared to the methods described by [127–129], the results show that HSV implemented with a standard image segmentation algorithm improves detection accuracy. According to the findings, HSV detection is completely reliable. The accuracy of CIELAB and YcbCr color space classifiers, used in the second and third stages of classification, dropped to the 9–10% range. According to the findings, the most effective method for detecting palm leaf tattering is image segmentation implemented in HSV color space.

6. Approach towards Healthy and Sustainable Production

The technologies and tools connected with precision farming related to palm oil monitoring have drawn the attention of many researchers. These resources and technologies provide a chance to comprehend and capitalize on the variabilities in the areas that have been recognized from the palm oil field owners; however, little emphasis has been applied until today. The following sub-sections give a brief overview of some of the deemed necessary steps that should be taken by the MPOB to increase the quality production of palm oil in the country.

6.1. Yield Monitoring Using UAV

The first step toward using precision agriculture in oil palm plantations is to quantify FFB from UAV stream images for return map creation. Autonomous UAVs have a number of benefits that make them ideal for use in yield tracking research, including a low price and lower price per mission flight. The purpose of this study is to evaluate the potential benefits of acquiring UAVs capable of flying over and inside oil palm plantations and collecting high-resolution detailed images from a variety of angles for the automatic creation of return maps. By using these maps, farmers will be able to better gauge how much water, fertilizer, and pesticides to use to ensure that their trees continue to thrive. Also useful for such a program are mobile robots outfitted with sensors and cameras, though this approach will not work for a large-size palm oil plantation [130]. A real-time machine-vision system could be developed for the accurate identification of the amount of FFB on the palm tree by using various sensor-based imaging and measurement techniques through each UAV. Having access to timely, accurate, and trustworthy data relevant to FFB in large-scale plantations is a critical need for the oil palm industry, and the industry should support making the development of such technology a priority [131].

6.2. Prediction Formulation

Oil palm farming occurs over a long time period, providing enough opportunity for studies of forecasting systems that can be applied at various points. Studies have shown that the current problem in agricultural oil palm is a significant gap between expected and realized yields [132]. However, this problem can be solved by using AI techniques in a wide variety of fields. Crop genotype, environmental conditions, and management practices are only a few of the variables that impact harvest success. Differences in crop yield from year to year and place to place are strongly influenced by geographical and temporal variations in environmental conditions. Producing food on a worldwide scale benefits greatly from knowing when to harvest, when to sow seeds, how much water will

be needed, what the cost will be, and how much food will grow. Accurate projections can thereby enable decisive factors for export and import processes.

6.3. Mechanized Fertilization

Soil nutrient deficiency is the most common agronomic barrier to increasing yields, but this can be easily overcome by applying a suitable quantity of fertilizers [133,134]. Therefore, it can be said that the cost of fertilizer plays a key role in the production of oil palms in Malaysia. It accounts for roughly 60–70% of the land used to support the cost of oil palms. Poor fertilization practices can result in significant monetary losses due to decreased harvests or overfertilization, which raises the risk of nutrient loss via runoff, birth control, and other methods [135]. The use of precision farming techniques appears to be an effective way to address these concerns. Keeping fertilization zones under control may help mitigate some of these shifts. However, the real opportunity to rethink fertilizer inputs lies in learning how to account for the enormous variation in fertilizer [136]. The key to improving efficiency is timing the fertilizer using specialized software, in addition to getting the fertilizer levels right and applying it in the right places. Soil erosion also reduces the nutrient value of fertilizer. Due to the difficulty in predicting tropical rainfall, the best times to apply fertilizers can be determined with the help of an expert system and artificial intelligence software [137].

6.4. Analyzing Fresh Fruit Bunch

To achieve the additional quantity and maintain oil quality required to meet international standards, it is necessary to sort and harvest oil palm FFB depending on its ripeness stage and other features before pressing. In order to guarantee a high oil extraction ratio (OER), oil palm harvest times are often determined by the fruit's maturity stage [132]. Since FFB is the primary by-product of oil palm farming, a great deal of attention has been paid to the possibility of using machine vision to assess factors such as fruit age, size, quality, etc. Therefore, the machine vision algorithm is crucial for determining the level of ripeness. As discussed in Section 5.1, different color space conversion, image processing functions and filters with thresholding can be used to develop dedicated algorithms to identify the ripeness of the fruit. Thereby, an AI-based deep learning model can be developed on convolutional networks that can assess to classify the quality of the fruit, whereby a set of fruit images will be fed to the convolutional network.

6.5. Web Monitoring and Virtual Plantation

Among the limitations of performing a study on palm oil plantations is the absence of precise data and enter variables for simulation and modelling functions. Unmanned aerial vehicle technology could be incorporated using image processing techniques for the three-dimensional renovation of their environment and creation of virtual plantations. The data extracted from the 3D models could lead to the evolution of dynamic web stock mapping and management systems. Otherwise, passive procedures, also called image-based renovation procedures (i.e., photogrammetry method), have been released using a normal camera and image detectors, which do not interfere with the reconstructed object. Within this method, a UAV armed with a regular RGB camera may collect images of the oil palm plantations from various views and angles. Computer software will then process these images to create a 3D version, and filter specific wavelengths to generate pictures that correspond to plant indicators and palm health. As an example, a reddish border image can describe nitrogen content and water pressure. The possibility of UAV picture data to simulate the physical process of palm photosynthesis as a consequence of different crown dimensions and densities intercepting various amounts of radiation could be evaluated using virtual plantations. A virtual farm may be employed to gauge palm height, height dimensions, and stock databases for creating dynamic Internet maps and yield forecast models. These maps may identify how different palm tree heights, crown sizes, density of plantations along with distribution patterns in various areas can impact

the water and fertilizer need. Moreover, mathematical models may be created based on the supported data from virtual plantations for estimating nitrogen demand and fertilizer application. Maps such as these help in providing precision-rich data for academic and educational purposes [138]. Researchers can access detailed measurements of palm and crown dimensions and the spacing between distinct palm trees, foliage area indices, and crown density as preliminary research for the possibility of autonomous harvesting.

7. Conclusions

The demand for palm oil from an ever-increasing population is on an increasing trend. Therefore, research efforts should be steered toward enhancing the performance of the industry, thereby reducing the negative environmental impact. Advanced remote sensing has an essential role in palm oil industry monitoring that has the capability to integrate the latest state-of-the-art AI technology. It is also useful for the evaluation of ecological as well as harvest conditions. The palm oil industry provides room for a dynamic shift that could be tailored with machine automation and methods of precision agriculture in order to bring a decrement in labor cost and thus improve productivity. Numerous palm oil plantation companies have initiated employing the latest technology and they also have a dedicated work unit for GIS/remote sensing systems equipped with state-of-the-art AI algorithms. Businesses can benefit greatly from utilizing remote sensing equipped with image-processing features in order to collect crucial information about the state of palm oil plantations, which in turn affects the outlook for the future of the company. Some methods have already been used, but they are not widely known about or published because their primary focus is not academic-oriented. The knowledge transfer of modern precision agriculture methods however requires more attention in order to advance in mutual benefit for the agricultural and industrial sectors, especially in light of the current era's rapid shift from Industry 3.0 to Industry 4.0. It is worth noting that Artificial intelligence (AI) has the potential to make a significant contribution to palm oil tree management by improving efficiency, reducing costs, and enhancing sustainability. Some ways AI can contribute to palm oil tree management include:

1. Yield prediction: AI algorithms can be used to predict yield based on factors such as tree size, age, and weather patterns, allowing for better planning and the optimization of production.
2. Pest and disease management: AI algorithms can be used to detect and predict pest and disease outbreaks, enabling early intervention and reducing crop losses.
3. Irrigation management: AI algorithms can be used to optimize irrigation systems by predicting water requirements based on soil moisture levels, weather patterns, and crop growth stages.
4. Harvest optimization: AI algorithms can be used to optimize the timing and process of harvesting, reducing costs and increasing efficiency.
5. Sustainability assessment: AI algorithms can be used to assess the sustainability of palm oil production, taking into account factors such as land use, water use, and carbon emissions, and providing recommendations for improvement.

In addition, more collaborative research on AI-based advanced remote sensing for oil palms between industry and academia needs to be carried out to provide a better understanding to fill the vacant gaps in this domain.

8. Future Work

The future of artificial intelligence in palm oil tree monitoring and health assessment looks promising. With advancements in aerial imagery and machine learning techniques, there is the potential for the more accurate and efficient monitoring of palm oil trees. Deep learning algorithms, such as convolutional neural networks (CNNs), have shown promising results in accurately classifying palm oil trees into healthy and unhealthy categories based on aerial imagery. In the future, the integration of AI and remote sensing technologies is expected to further improve palm oil tree monitoring and health assessment. For example,

the use of drones equipped with high-resolution cameras and sensors can provide real-time data on palm oil tree health, leading to more efficient and effective decision-making. Additionally, AI algorithms can be used to analyze large amounts of data and identify patterns, providing insights into factors that affect palm oil tree health, such as pests and diseases, water stress, and nutrient deficiencies.

Overall, the future of AI in palm oil tree monitoring and health assessment holds great potential for improving the sustainability and productivity of palm oil production. It will be important for the industry to continue investing in AI research and development to fully realize its potential in this area.

Author Contributions: Conceptualization, M.N.A. and E.A.; Formal analysis, M.N.A., E.A. and E.A.B.; Funding acquisition, S.S.N.A.; Methodology, M.N.A. and E.A.B.; Project administration, E.A.B. and S.S.N.A.; Supervision, E.A.B. and S.S.N.A.; Writing—original draft, M.N.A.; Writing—review and editing, M.N.A. and E.A. All authors have read and agreed to the published version of the manuscript.

Funding: This study was funded by Research Creativity and Management Office, Universiti Sains Malaysia using the grant JRS SATU 304/PAERO/6315715.

Institutional Review Board Statement: Not applicable.

Informed Consent Statement: Not applicable.

Data Availability Statement: Not applicable.

Acknowledgments: The authors would like to acknowledge the support from the School of Aerospace Engineering, Universiti Sains Malaysia and the School of Electrical and Electronics Engineering, Universiti Sains Malaysia to conduct this review.

Conflicts of Interest: The authors declare no conflict of interest.

References

1. Ibrahim, I.; Awang, A.H.; Hashim, K.; Ramli, Z.; Lyndon, N.; Azian, F.U.M.; Hamid, M.H.A. *Independent Oil Palm Smallholder Participation and Technology Transfer Selected Topics on Archaeology, History and Culture in the Malay World*; Springer: Berlin/Heidelberg, Germany, 2018; pp. 217–224.
2. Oettli, P.; Behera, S.K.; Yamagata, T. Climate Based Predictability of Oil Palm Tree Yield in Malaysia. *Sci. Rep.* **2018**, *8*, 2271. [CrossRef] [PubMed]
3. Umar, M.S.; Urmee, T.; Jennings, P. A policy framework and industry roadmap model for sustainable oil palm biomass electricity generation in Malaysia. *Renew. Energy* **2018**, *128*, 275–284. [CrossRef]
4. Rizeei, H.M.; Shafri, H.Z.M.; Mohamoud, M.A.; Pradhan, B.; Kalantar, B. Oil Palm Counting and Age Estimation from WorldView-3 Imagery and LiDAR Data Using an Integrated OBIA Height Model and Regression Analysis. *J. Sens.* **2018**, *2018*, 2536327. [CrossRef]
5. Moreno-Peñaranda, R.; Gasparatos, A.; Stromberg, P.; Suwa, A.; de Oliveira, J.A.P. *Stakeholder Perceptions of the Eco-system Services and Human Well-Being Impacts of Palm Oil Biofuels in Indonesia and Malaysia Biofuels and Sustainability*; Springer: Berlin/Heidelberg, Germany, 2018; pp. 133–173.
6. Cheng, Y.; Yu, L.; Xu, Y.; Liu, X.; Lu, H.; Cracknell, A.P.; Kanniah, K.; Gong, P. Towards global oil palm plantation mapping using remote-sensing data. *Int. J. Remote Sens.* **2018**, *39*, 5891–5906. [CrossRef]
7. Najib, N.E.M.; Kanniah, K.D. Optical and radar remote sensing data for forest cover mapping in Peninsular Malaysia. *Singap. J. Trop. Geogr.* **2018**, *40*, 272–290. [CrossRef]
8. Wang, Y.; Zhu, X.; Wu, B. Automatic detection of individual oil palm trees from UAV images using HOG features and an SVM classifier. *Int. J. Remote Sens.* **2018**, *40*, 7356–7370. [CrossRef]
9. Daliman, S.; Kamal, N.S.M.; Ahmad, S. Development of GUI For Automated Oil Palm Tree Counting Based on Remote Sensing Imagery. In Proceedings of the 2018 International Conference on Smart Computing and Electronic Enterprise (ICSCEE), Shah Alam, Malaysia, 11–12 July 2018.
10. Vargas, L.; Willemen, L.; Hein, L. Assessing the Capacity of Ecosystems to Supply Ecosystem Services Using Remote Sensing and An Ecosystem Accounting Approach. *Environ. Manag.* **2018**, *63*, 1–15. [CrossRef]
11. Ahmed, G.B.; Shariff, A.; Balasundram, S.; Abdullah, A. Estimation of soil loss in Seremban, Malaysia using GIS and remote sensing technique. In Proceedings of the Paper presented at the IOP Conference Series: Earth and Environmental Science, Kuala Lumpur, Malaysia, 24–25 April 2018.
12. Kee, Y.; Shariff, A.; Sood, A.; Nordin, L. Application of SAR data for oil palm tree discrimination. In Proceedings of the Conference Series: Earth and Environmental Science, Kuala Lumpur, Malaysia, 24–25 April 2018.

13. Estes, L.; Chen, P.; Debats, S.; Evans, T.; Ferreira, S.; Kuemmerle, T.; Wood, E. A large-area, spatially continuous as-sessment of land cover map error and its impact on downstream analyses. *Glob. Chang. Biol.* **2018**, *24*, 322–337. [CrossRef]
14. Matysek, M.; Evers, S.; Samuel, M.K.; Sjogersten, S. High heterotrophic CO 2 emissions from a Malaysian oil palm plan-tations during dry-season. *Wetl. Ecol. Manag.* **2018**, *26*, 415–424. [CrossRef]
15. Hasmadi, M.; Pakhriazad, H.; Shahrin, M. Evaluating supervised and unsupervised techniques for land cover mapping using remote sensing data. *Geogr. Malays. J. Soc. Space* **2017**, *5*, 1–10.
16. Ayele, G.T.; Tebeje, A.K.; Demissie, S.S.; Belete, M.A.; Jemberrie, M.; Teshome, W.M.; Mengistu, D.T.; Teshale, E.Z. Time Series Land Cover Mapping and Change Detection Analysis Using Geographic Information System and Remote Sensing, Northern Ethiopia. *Air Soil Water Res.* **2018**, *11*, 1178–6221. [CrossRef]
17. Sun, Z.; Di, L.; Fang, H. Using long short-term memory recurrent neural network in land cover classification on Landsat and Cropland data layer time series. *Int. J. Remote Sens.* **2018**, *40*, 593–614. [CrossRef]
18. Singh, S.K.; Laari, P.B.; Mustak, S.; Srivastava, P.K.; Szabó, S. Modelling of land use land cover change using earth ob-servation data-sets of Tons River Basin, Madhya Pradesh, India. *Geocarto Int.* **2018**, *33*, 1202–1222. [CrossRef]
19. Lv, Z.; Liu, T.; Wan, Y.; Benediktsson, J.A.; Zhang, X. Post-Processing Approach for Refining Raw Land Cover Change Detection of Very High-Resolution Remote Sensing Images. *Remote Sens.* **2018**, *10*, 472. [CrossRef]
20. Li, X.; Ling, F.; Foody, G.M.; Ge, Y.; Zhang, Y.; Du, Y. Generating a series of fine spatial and temporal resolution land cover maps by fusing coarse spatial resolution remotely sensed images and fine spatial resolution land cover maps. *Remote Sens. Environ.* **2017**, *196*, 293–311. [CrossRef]
21. Cheng, Y.; Yu, L.; Cracknell, A.P.; Gong, P. Oil palm mapping using Landsat and PALSAR: A case study in Malaysia. *Int. J. Remote Sens.* **2016**, *37*, 5431–5442. [CrossRef]
22. Alonzo, M.; Bookhagen, B.; Roberts, D.A. Urban tree species mapping using hyperspectral and lidar data fusion. *Remote Sens. Environ.* **2014**, *148*, 70–83. [CrossRef]
23. Rosenbaum, D.; Leitloff, J.; Kurz, F.; Meynberg, O.; Reize, T. Real-time image processing for road traffic data extraction from aerial images. In Proceedings of the ISPRS Technical Commission VII Symposium 2010, Vienna, Austria, 5–7 July 2010.
24. Roessner, S.; Segl, K.; Heiden, U.; Kaufmann, H. Automated differentiation of urban surfaces based on airborne hyper-spectral imagery. *IEEE Trans. Geosci. Remote Sens.* **2001**, *39*, 1525–1532. [CrossRef]
25. Puissant, A.; Rougier, S.; Stumpf, A. Object-oriented mapping of urban trees using Random Forest classifiers. *Int. J. Appl. Earth Obs. Geoinf.* **2014**, *26*, 235–245. [CrossRef]
26. Wania, A.; Weber, C. Hyperspectral imagery and urban green observation. In Proceedings of the 2007 Urban Remote Sensing Joint Event, Paris, France, 11–13 April 2007.
27. Kneissl, T.; van Gasselt, S.; Neukum, G. Map-projection-independent crater size-frequency determination in GIS envi-ronments—New software tool for ArcGIS. *Planet. Space Sci.* **2011**, *59*, 1243–1254. [CrossRef]
28. Cigna, F.; Osmanoğlu, B.; Cabral-Cano, E.; Dixon, T.H.; Ávila-Olivera, J.A.; Garduño-Monroy, V.H.; DeMets, C.; Wdowinski, S. Monitoring land subsidence and its induced geological hazard with Synthetic Aperture Radar Interferometry: A case study in Morelia, Mexico. *Remote Sens. Environ.* **2012**, *117*, 146–161. [CrossRef]
29. Huang, H.; Chen, Y.; Clinton, N.; Wang, J.; Wang, X.; Liu, C.; Gong, P.; Yang, J.; Bai, Y.; Zheng, Y.; et al. Mapping major land cover dynamics in Beijing using all Landsat images in Google Earth Engine. *Remote Sens. Environ.* **2017**, *202*, 166–176. [CrossRef]
30. Glinskis, E.A.; Gutiérrez-Vélez, V.H. Quantifying and understanding land cover changes by large and small oil palm expansion regimes in the Peruvian Amazon. *Land Use Policy* **2018**, *80*, 95–106. [CrossRef]
31. Wai, K.; Wang, X.; Lin, T.; Wong, M.; Zeng, S.; He, N.; Wang, D. Observational evidence of a long-term increase in pre-cipitation due to urbanization effects and its implications for sustainable urban living. *Sci. Total Environ.* **2017**, *599*, 647–654. [CrossRef]
32. Frohn, R.C.; Lopez, R.D. *Remote Sensing for Landscape Ecology: New Metric Indicators: Monitoring, Modeling, and Assessment of Ecosystems*; CRC Press: Boca Raton, FL, USA, 2017.
33. Pettorelli, N.; Wegmann, M.; Skidmore, A.; Mücher, S.; Dawson, T.P.; Fernandez, M.; Lucas, R.; Schaepman, M.E.; Wang, T.; O'Connor, B.; et al. Framing the concept of satellite remote sensing essential biodiversity variables: Challenges and future directions. *Remote Sens. Ecol. Conserv.* **2016**, *2*, 122–131. [CrossRef]
34. Vu, T.-T.; Thy, P.T.M.; Nguyen, L. Multiscale remote sensing of urbanization in Ho Chi Minh city, Vietnam—A focused study of the south. *Appl. Geogr.* **2018**, *92*, 168–181. [CrossRef]
35. Liu, H.; An, H. Analysis of the importance of five new spectral indices from WorldView-2 in tree species classifica-tion. *J. Spat. Sci.* **2018**, *65*, 455–466. [CrossRef]
36. Huang, B.; Zhao, B.; Song, Y. Urban land-use mapping using a deep convolutional neural network with high spatial res-olution multispectral remote sensing imagery. *Remote Sens. Environ.* **2018**, *214*, 73–86. [CrossRef]
37. Li, W.; Fu, H.; Yu, L.; Cracknell, A. Deep Learning Based Oil Palm Tree Detection and Counting for High-Resolution Remote Sensing Images. *Remote Sens.* **2016**, *9*, 22. [CrossRef]
38. Chen, Q.; Lu, D.; Keller, M.; Dos-Santos, M.N.; Bolfe, E.L.; Feng, Y.; Wang, C. Modeling and Mapping Agroforestry Aboveground Biomass in the Brazilian Amazon Using Airborne Lidar Data. *Remote Sens.* **2015**, *8*, 21. [CrossRef]
39. Upgupta, S.; Singh, S.; Tiwari, P.S. Estimation of Aboveground Phytomass of Plantations Using Digital Photogrammetry and High Resolution Remote Sensing Data. *J. Indian Soc. Remote Sens.* **2014**, *43*, 311–323. [CrossRef]

40. Lakshmi, K.D.; Vaithiyanathan, V. Image Registration Techniques Based on the Scale Invariant Feature Transform. *IETE Tech. Rev.* **2016**, *34*, 22–29. [CrossRef]
41. Plowright, A.A.; Coops, N.C.; Chance, C.M.; Sheppard, S.R.; Aven, N.W. Multi-scale analysis of relationship between imperviousness and urban tree height using airborne remote sensing. *Remote Sens. Environ.* **2017**, *194*, 391–400. [CrossRef]
42. Srestasathiern, P.; Siripon, S.; Wasuhiranyrith, R.; Kooha, P.; Moukomla, S. Estimating above ground biomass for eucalyptus plantation using data from unmanned aerial vehicle imagery. *Remote Sens. Agric. Ecosyst. Hydrol.* **2018**, *10783*, 1078308. [CrossRef]
43. Shaharum, N.S.N.; Shafri, H.Z.M.; Ghani, W.A.W.A.K.; Samsatli, S.; Yusuf, B.; Al-Habshi, M.M.A.; Prince, H.M. Image classification for mapping oil palm distribution via support vector machine using scikit-learn module. *ISPRS Int. Arch. Photogramm. Remote Sens. Spat. Inf. Sci.* **2018**, *XLII-4/W9*, 133–137. [CrossRef]
44. Csillik, O.; Cherbini, J.; Johnson, R.; Lyons, A.; Kelly, M. Identification of Citrus Trees from Unmanned Aerial Vehicle Imagery Using Convolutional Neural Networks. *Drones* **2018**, *2*, 39. [CrossRef]
45. Zhu, J.; Sun, K.; Jia, S.; Li, Q.; Hou, X.; Lin, W.; Liu, B.; Qiu, G. Urban Traffic Density Estimation Based on Ultrahigh-Resolution UAV Video and Deep Neural Network. *IEEE J. Sel. Top. Appl. Earth Obs. Remote Sens.* **2018**, *11*, 4968–4981. [CrossRef]
46. Djerriri, K.; Ghabi, M.; Karoui, M.S.; Adjoudj, R. Palm Trees Counting in Remote Sensing Imagery Using Regression Convolutional Neural Network. In Proceedings of the IGARSS 2018–2018 IEEE International Geoscience and Remote Sensing Symposi-um, Valencia, Spain, 1 July 2018.
47. Cheang, E.K.; Cheang, T.K.; Tay, Y.H. Using Convolutional Neural Networks to Count Palm Trees in Satellite Images. *arXiv* **2017**, arXiv:1701.06462.
48. Nogueira, K.; Penatti, O.A.; dos Santos, J.A. Towards better exploiting convolutional neural networks for remote sensing scene classification. *Pattern Recognit.* **2017**, *61*, 539–556. [CrossRef]
49. Robinson, J.P.; Fu, Y. Pre-trained D-CNN models for detecting complex events in unconstrained videos. *Sens. Anal. Technol. Biomed. Cogn. Appl.* **2016**, *9871*, 191–199.
50. Zhou, Z.; Wang, H.; Shang, W.; Zhang, L. Image Segmentation Algorithms Based on Convolutional Neural Networks. In Proceedings of the 2018 IEEE/ACIS 17th International Conference on Computer and Information Science (ICIS), Singapore, 6–8 June 2018.
51. Bertrand, S.; Cerutti, G.; Tougne, L. Visualization of Leaf Botanical Features Extracted from AlexNet Convolutional Layers. In Proceedings of the the IAMPS-International Workshop on Image Analysis Methods for the Plant Sciences, Nottingham, UK, 22–23 January 2018.
52. Castelluccio, M.; Poggi, G.; Sansone, C.; Verdoliva, L. Training convolutional neural networks for semantic classification of remote sensing imagery. In Proceedings of the 2017 Joint Urban Remote Sensing Event (JURSE), Dubai, United Arab Emirates, 6–8 March 2017. [CrossRef]
53. Cheng, G.; Li, Z.; Yao, X.; Guo, L.; Wei, Z. Remote Sensing Image Scene Classification Using Bag of Convolutional Features. *IEEE Geosci. Remote Sens. Lett.* **2017**, *14*, 1735–1739. [CrossRef]
54. Madry, S.; Martinez, P.; Laufer, R. *Smallsats for Remote Sensing–The Swarm Is Here! Innovative Design, Manufacturing and Testing of Small Satellites*; Springer: Berlin/Heidelberg, Germany, 2018; pp. 31–42.
55. Souri, A.H.; Choi, Y.; Jeon, W.; Woo, J.H.; Zhang, Q.; Kurokawa, J.I. Remote sensing evidence of decadal changes in major tropospheric ozone precursors over East Asia. *J. Geophys. Res. Atmos.* **2017**, *122*, 2474–2492. [CrossRef]
56. Schweiger, A.K.; Schütz, M.; Risch, A.C.; Kneubühler, M.; Haller, R.; Schaepman, M.E. How to predict plant functional types using imaging spectroscopy: Linking vegetation community traits, plant functional types and spectral response. *Methods Ecol. Evol.* **2017**, *8*, 86–95. [CrossRef]
57. Nevalainen, O.; Honkavaara, E.; Tuominen, S.; Viljanen, N.; Hakala, T.; Yu, X.; Hyyppä, J.; Saari, H.; Pölönen, I.; Imai, N.N.; et al. Individual Tree Detection and Classification with UAV-Based Photogrammetric Point Clouds and Hyperspectral Imaging. *Remote Sens.* **2017**, *9*, 185. [CrossRef]
58. Wang, L.; Zhang, J.; Liu, P.; Choo, K.-K.R.; Huang, F. Spectral–spatial multi-feature-based deep learning for hyperspectral remote sensing image classification. *Soft Comput.* **2016**, *21*, 213–221. [CrossRef]
59. Yuan, H.; Yang, G.; Li, C.; Wang, Y.; Liu, J.; Yu, H.; Feng, H.; Xu, B.; Zhao, X.; Yang, X. Retrieving Soybean Leaf Area Index from Unmanned Aerial Vehicle Hyperspectral Remote Sensing: Analysis of RF, ANN, and SVM Regression Models. *Remote Sens.* **2017**, *9*, 309. [CrossRef]
60. Poland, T.M.; Rassati, D. Improved biosecurity surveillance of non-native forest insects: A review of current methods. *J. Pest Sci.* **2018**, *92*, 37–49. [CrossRef]
61. Gouveia, C.; Trigo, R.; Beguería, S.; Vicente-Serrano, S. Drought impacts on vegetation activity in the Mediterranean region: An assessment using remote sensing data and multi-scale drought indicators. *Glob. Planet. Chang.* **2017**, *151*, 15–27. [CrossRef]
62. Andreu-Hayles, L.; Gaglioti, B.V.; D'Arrigo, R.; Anchukaitis, K.J.; Goetz, S. *Shrub Sensitivity to Recent Warming across Arctic Alaska from Dendrochronological and Remote Sensing Records*; EGU General Assembly Conference Abstracts: Vienna, Austria, 2017.
63. Mariano, D.A.; dos Santos, C.A.; Wardlow, B.D.; Anderson, M.C.; Schiltmeyer, A.V.; Tadesse, T.; Svoboda, M.D. Use of remote sensing indicators to assess effects of drought and human-induced land degradation on ecosystem health in Northeastern Brazil. *Remote Sens. Environ.* **2018**, *213*, 129–143. [CrossRef]
64. Campos, I.; González-Gómez, L.; Villodre, J.; González-Piqueras, J.; Suyker, A.E.; Calera, A. Remote sensing-based crop biomass with water or light-driven crop growth models in wheat commercial fields. *Field Crop. Res.* **2018**, *216*, 175–188. [CrossRef]

65. Valderrama-Landeros, L.; Flores-De-Santiago, F.; Kovacs, J.M.; Flores-Verdugo, F. An assessment of commonly employed satellite-based remote sensors for mapping mangrove species in Mexico using an NDVI-based classification scheme. *Environ. Monit. Assess.* **2017**, *190*, 23. [CrossRef]
66. Hakkenberg, C.; Zhu, K.; Peet, R.; Song, C. Mapping multi-scale vascular plant richness in a forest landscape with inte-grated LiDAR and hyperspectral remote-sensing. *Ecology* **2018**, *99*, 474–487. [CrossRef]
67. Al Shidi, R.; Kumar, L.; Al-Khatri, S.; Albahri, M.; Alaufi, M. Relationship of date palm tree density to Dubas bug Om-matissus lybicus infestation in Omani orchards. *Agriculture* **2018**, *8*, 64. [CrossRef]
68. Savelli, A.; Atieno, M.O.; Giles, J.; Santos, J.; Leyte, J.; Nguyen, N.V.B.; Grosjean, G. Climate-Smart Agriculture in Indonesia. In *CSA Country Profiles for Asia Series*; The World Bank Group: Washington, DC, USA, 2021.
69. Cheng, Y.; Yu, L.; Xu, Y.; Lu, H.; Cracknell, A.P.; Kanniah, K.; Gong, P. Mapping oil palm extent in Malaysia using ALOS-2 PALSAR-2 data. *Int. J. Remote Sens.* **2017**, *39*, 432–452. [CrossRef]
70. Yarak, K.; Witayangkurn, A.; Kritiyutanont, K.; Arunplod, C.; Shibasaki, R. Oil Palm Tree Detection and Health Classification on High-Resolution Imagery Using Deep Learning. *Agriculture* **2021**, *11*, 183. [CrossRef]
71. Wibowo, H.; Sitanggang, I.S.; Mushthofa, M.; Adrianto, H.A. Large-Scale Oil Palm Trees Detection from High-Resolution Remote Sensing Images Using Deep Learning. *Big Data Cogn. Comput.* **2022**, *6*, 89. [CrossRef]
72. Ong, J.H.; Ong, P.; Woon, K.L. Image-Based Oil Palm Leaves Disease Detection Using Convolutional Neural Network. *J. Inf. Commun. Technol.* **2022**, *21*, 383–410. [CrossRef]
73. Réjou-Méchain, M.; Tanguy, A.; Piponiot, C.; Chave, J.; Hérault, B. biomass: An r package for estimating above-ground biomass and its uncertainty in tropical forests. *Methods Ecol. Evol.* **2017**, *8*, 1163–1167. [CrossRef]
74. Asari, N.; Suratman, M.N.; Jaafar, J. Modelling and mapping of above ground biomass (AGB) of oil palm plantations in Malaysia using remotely-sensed data. *Int. J. Remote Sens.* **2017**, *38*, 4741–4764. [CrossRef]
75. He, A.; McDermid, G.J.; Rahman, M.M.; Strack, M.; Saraswati, S.; Xu, B. Developing Allometric Equations for Estimating Shrub Biomass in a Boreal Fen. *Forests* **2018**, *9*, 569. [CrossRef]
76. Huff, S.; Ritchie, M.; Temesgen, H. Allometric equations for estimating aboveground biomass for common shrubs in northeastern California. *For. Ecol. Manag.* **2017**, *398*, 48–63. [CrossRef]
77. Basuki, I.; Kauffman, J.B.; Peterson, J.; Anshari, G.; Murdiyarso, D. Land cover changes reduce net primary production in tropical coastal peatlands of West Kalimantan, Indonesia. *Mitig. Adapt. Strateg. Glob. Chang.* **2019**, *24*, 557–573. [CrossRef]
78. Gibbs, J.A.; Pound, M.; French, A.P.; Wells, D.M.; Murchie, E.; Pridmore, T. Approaches to three-dimensional recon-struction of plant shoot topology and geometry. *Funct. Plant Biol.* **2017**, *44*, 62–75. [CrossRef] [PubMed]
79. Alexander, C.; Korstjens, A.H.; Hill, R.A. Influence of micro-topography and crown characteristics on tree height esti-mations in tropical forests based on LiDAR canopy height models. *Int. J. Appl. Earth Obs. Geoinf.* **2018**, *65*, 105–113.
80. Mielcarek, M.; Stereńczak, K.; Khosravipour, A. Testing and evaluating different LiDAR-derived canopy height model generation methods for tree height estimation. *Int. J. Appl. Earth Obs. Geoinf.* **2018**, *71*, 132–143. [CrossRef]
81. Budei, B.C.; St-Onge, B. Variability of Multispectral Lidar 3D and Intensity Features with Individual Tree Height and Its Influence on Needleleaf Tree Species Identification. *Can. J. Remote Sens.* **2018**, *44*, 263–286. [CrossRef]
82. Wanik, D.; Parent, J.; Anagnostou, E.; Hartman, B. Using vegetation management and LiDAR-derived tree height data to improve outage predictions for electric utilities. *Electr. Power Syst. Res.* **2017**, *146*, 236–245. [CrossRef]
83. Su, Y.; Ma, Q.; Guo, Q. Fine-resolution forest tree height estimation across the Sierra Nevada through the integration of spaceborne LiDAR, airborne LiDAR, and optical imagery. *Int. J. Digit. Earth* **2015**, *10*, 307–323. [CrossRef]
84. Nunes, M.H.; Ewers, R.M.; Turner, E.C.; Coomes, D.A. Mapping aboveground carbon in oil palm plantations using LiDAR: A comparison of tree-centric versus area-based approaches. *Remote Sens.* **2017**, *9*, 816. [CrossRef]
85. Coops, N.C.; Tompalski, P.; Goodbody, T.R.; Queinnec, M.; Luther, J.E.; Bolton, D.K.; White, J.C.; Wulder, M.A.; van Lier, O.R.; Hermosilla, T. Modelling lidar-derived estimates of forest attributes over space and time: A review of approaches and future trends. *Remote Sens. Environ.* **2021**, *260*, 112477. [CrossRef]
86. Gao, L.; Shi, W.; Zhu, J.; Shao, P.; Sun, S.; Li, Y.; Wang, F.; Gao, F. Novel Framework for 3D Road Extraction Based on Airborne LiDAR and High-Resolution Remote Sensing Imagery. *Remote Sens.* **2021**, *13*, 4766. [CrossRef]
87. Coops, N.C.; Tompalski, P.; Goodbody, T.R.H.; Achim, A.; Mulverhill, C. Framework for near real-time forest inventory using multi source remote sensing data. *For. Int. J. For. Res.* **2022**, *96*, 1–19. [CrossRef]
88. Perez, R.P.; Costes, E.; Théveny, F.; Griffon, S.; Caliman, J.-P.; Dauzat, J. 3D plant model assessed by terrestrial LiDAR and hemispherical photographs: A useful tool for comparing light interception among oil palm progenies. *Agric. For. Meteorol.* **2018**, *249*, 250–263. [CrossRef]
89. Burton, M.E.H.; Poulsen, J.R.; Lee, M.E.; Medjibe, V.P.; Stewart, C.G.; Venkataraman, A.; White, L.J.T. Reducing Carbon Emissions from Forest Conversion for Oil Palm Agriculture in Gabon. *Conserv. Lett.* **2016**, *10*, 297–307. [CrossRef]
90. Sinha, S.; Jeganathan, C.; Sharma, L.; Nathawat, M. A review of radar remote sensing for biomass estimation. *Int. J. Environ. Sci. Technol.* **2015**, *12*, 1779–1792. [CrossRef]
91. Schepaschenko, D.; Moltchanova, E.; Shvidenko, A.; Blyshchyk, V.; Dmitriev, E.; Martynenko, O.; See, L.; Kraxner, F. Improved Estimates of Biomass Expansion Factors for Russian Forests. *Forests* **2018**, *9*, 312. [CrossRef]

92. Corbane, C.; Lang, S.; Pipkins, K.; Alleaume, S.; Deshayes, M.; Millán, V.E.G.; Strasser, T.; Borre, J.V.; Toon, S.; Michael, F. Remote sensing for mapping natural habitats and their conservation status—New opportunities and challenges. *Int. J. Appl. Earth Obs. Geoinf.* **2015**, *37*, 7–16. [CrossRef]
93. Ma, J.; Du, K.; Zheng, F.; Zhang, L.; Gong, Z.; Sun, Z. A recognition method for cucumber diseases using leaf symptom images based on deep convolutional neural network. *Comput. Electron. Agric.* **2018**, *154*, 18–24. [CrossRef]
94. Pohl, C.; Chong, K.; van Genderen, J. Multisensor Approach to Oil Palm Plantation Monitoring Using Data Fusion and GIS. In Proceedings of the 36th Asian Conference on Remote Sensing 'Fostering Resiient Growth in Asia', Manila, Philippines, 24–28 October 2015.
95. Villard, L.; Le Toan, T.; Minh, D.H.T.; Mermoz, S.; Bouvet, A. *Forest Biomass from Radar Remote Sensing Land Surface Remote Sensing in Agriculture and Forest*; Elsevier: Amsterdam, The Netherlands, 2017; pp. 363–425.
96. Popescu, S.; Zhou, T.; Nelson, R.; Neuenschwander, A.; Sheridan, R.; Narine, L.; Walsh, K. Photon counting LiDAR: An adaptive ground and canopy height retrieval algorithm for ICESat-2 data. *Remote Sens. Environ.* **2018**, *208*, 154–170. [CrossRef]
97. James, M.; Robson, S.; D'Oleire-Oltmanns, S.; Niethammer, U. Optimising UAV topographic surveys processed with structure-from-motion: Ground control quality, quantity and bundle adjustment. *Geomorphology* **2017**, *280*, 51–66. [CrossRef]
98. Kalacska, M.; Chmura, G.L.; Lucanus, O.; Bérubé, D.; Arroyo-Mora, J.P. Structure from motion will revolutionize analyses of tidal wetland landscapes. *Remote Sens. Environ.* **2017**, *199*, 14–24. [CrossRef]
99. Panagiotidis, D.; Abdollahnejad, A.; Surový, P.; Chiteculo, V. Determining tree height and crown diameter from high-resolution UAV imagery. *Int. J. Remote Sens.* **2016**, *38*, 2392–2410. [CrossRef]
100. Torres, G.; Sarria, G.; Martinez, G.; Varon, F.; Drenth, A.; Guest, D. Bud rot caused by Phytophthora palmivora: A de-structive emerging disease of oil palm. *Phytopathology* **2016**, *106*, 320–329. [CrossRef] [PubMed]
101. Costa, O.Y.D.A.; Tupinambá, D.D.; Bergmann, J.C.; Barreto, C.C.; Quirino, B.F. Fungal diversity in oil palm leaves showing symptoms of Fatal Yellowing disease. *PLoS ONE* **2018**, *13*, e0191884. [CrossRef]
102. Azlan, A.M.N.; Ahmad, Z.A.M.; Idris, A.S.; Vadamalai, G. Assessment of Leaf Spot and Anthracnose Diseases in Nurseries and It Relationship with Oil Palm Seedling Ages. *Int. J. Adv. Multidiscip. Res.* **2018**, *5*, 19–26.
103. Khaled, A.Y.; Abd Aziz, S.; Bejo, S.K.; Nawi, N.M.; Abu Seman, I. Spectral features selection and classification of oil palm leaves infected by Basal stem rot (BSR) disease using dielectric spectroscopy. *Comput. Electron. Agric.* **2018**, *144*, 297–309. [CrossRef]
104. Nurdiansyah, F.; Clough, Y.; Wiegand, K.; Tscharntke, T. Local and Landscape Management Effects on Pests, Diseases, Weeds and Biocontrol in Oil Palm Plantations-A Review. Local and Landscape Management of Biological Pest Control in Oil Palm Plantations. Ph.D. Thesis, Georg-August University, Germany, Göttingen, 2016.
105. Suwannarach, N.; Kumla, J.; Lumyong, S. First report of Alternaria leaf blight disease on oil palm caused by Alternaria longipes in Thailand. *Phytoparasitica* **2014**, *43*, 57–59. [CrossRef]
106. Izzuddin, M.; Nisfariza, M.; Ezzati, B.; Idris, A.; Steven, M.; Boyd, D. Analysis of Airborne Hyperspectral Image Using Vegetation Indices, Red Edge Position and Continuum Removal for Detection of Ganoderma Disease in Oil Palm. *J. Oil Palm Res.* **2018**, *30*, 416–428.
107. Ahmad, N.; Hasan, Z.A.A.; Muhamad, H.; Bilal, S.H.; Yusof, N.Z.; Idris, Z. Determination of Total Phenol, Flavonoid, Antioxidant Activity of Oil Palm Leaves Extracts and Their Application in Trans-Parent Soap. *J. Oil Palm Res.* **2018**, *30*, 315–325.
108. Olafisoye, O.B.; Oguntibeju, O.O.; Osibote, O.A. Trace elements and radionuclides in palm oil, soil, water, and leaves from oil palm plantations: A review. *Crit. Rev. Food Sci. Nutr.* **2017**, *57*, 1295–1315. [CrossRef]
109. Smith, T.E.L.; Evers, S.; Yule, C.M.; Gan, J.Y. In Situ Tropical Peatland Fire Emission Factors and Their Variability, as Determined by Field Measurements in Peninsula Malaysia. *Glob. Biogeochem. Cycles* **2018**, *32*, 18–31. [CrossRef]
110. Tong, Y.-S. Vertical specialisation or linkage development for agro-commodity value chain upgrading?The case of Malaysian palm oil. *Land Use Policy* **2017**, *68*, 585–596. [CrossRef]
111. Oviasogie, P.; Ikuenobe, C.; Ugbah, M.; Imogie, A.; Ekhator, F.; Oko-Oboh, E.; Edokpayi, A. *A Review of Study on Ferti-lizer Response by the Oil Palm (Elaeis guineensis) in Nigeria Improving the Profitability, Sustainability and Efficiency of Nutrients through Site Specific Fertilizer Recommendations in West Africa Agro-Ecosystems*; Springer: Berlin/Heidelberg, Germany, 2018; pp. 301–323.
112. Woittiez, L.S.; van Wijk, M.T.; Slingerland, M.; van Noordwijk, M.; Giller, K.E. Yield gaps in oil palm: A quantitative review of contributing factors. *Eur. J. Agron.* **2017**, *83*, 57–77. [CrossRef]
113. Singh, V.; Misra, A. Detection of plant leaf diseases using image segmentation and soft computing techniques. *Inf. Process. Agric.* **2017**, *4*, 41–49. [CrossRef]
114. Arya, M.S.; Anjali, K.; Unni, D. Detection of unhealthy plant leaves using image processing and genetic algorithm with Arduino. In Proceedings of the 2018 International Conference on Power, Signals, Control and Computation (EPSCICON), Thrissur, India, 6–10 January 2018. [CrossRef]
115. Sahoo, R.K.; Panda, R.; Barik, R.C.; Panda, S.N. Automatic Dead Zone Detection in 2-D Leaf Image Using Clustering and Segmentation Technique. *Int. J. Image Graph. Signal Process* **2018**, *10*, 11–30. [CrossRef]
116. Bai, X.; Li, X.; Fu, Z.; Lv, X.; Zhang, L. A fuzzy clustering segmentation method based on neighborhood grayscale in-formation for defining cucumber leaf spot disease images. *Comput. Electron. Agric.* **2017**, *136*, 157–165. [CrossRef]
117. Danisman, T.; Bilasco, I.M.; Martinet, J.; Djeraba, C. Intelligent pixels of interest selection with application to facial ex-pression recognition using multilayer perceptron. *Signal Process.* **2013**, *93*, 1547–1556. [CrossRef]

118. Jolliffe, I.T.; Cadima, J. Principal component analysis: A review and recent developments. *Philos. Trans. R. Soc. A Math. Phys. Eng. Sci.* **2016**, *374*, 20150202. [CrossRef]
119. Demšar, U.; Harris, P.; Brunsdon, C.; Fotheringham, A.S.; McLoone, S. Principal Component Analysis on Spatial Data: An Overview. *Ann. Assoc. Am. Geogr.* **2013**, *103*, 106–128. [CrossRef]
120. Senthilkumaran, N.; Vaithegi, S. Image segmentation by using thresholding techniques for medical images. *Comput. Sci. Eng. Int. J.* **2016**, *6*, 1–13.
121. Firdousi, R.; Parveen, S. Local Thresholding Techniques in Image Binarization. *Int. J. Eng. Comput. Sci.* **2014**, *3*, 4062–4065.
122. Wang, W.; Duan, L.; Wang, Y. Fast Image Segmentation Using Two-Dimensional Otsu Based on Estimation of Distribution Algorithm. *J. Electr. Comput. Eng.* **2017**, *2017*, 1735176. [CrossRef]
123. Ali, M.; Siarry, P.; Pant, M. Multi-level Image Thresholding Based on Hybrid Differential Evolution Algorithm. Application on Medical Images. *Metaheuristics Med. Biol.* **2017**, *704*, 23–36. [CrossRef]
124. Xiao, Y.; Cao, Z.; Yuan, J. Entropic image thresholding based on GLGM histogram. *Pattern Recognit. Lett.* **2014**, *40*, 47–55. [CrossRef]
125. Sweeney, C.; Liu, L.; Arietta, S.; Lawrence, J. *HIPI: A Hadoop Image Processing Interface for Image-Based Mapreduce Tasks*; University of Virginia: Charlottesville, VA, USA, 2011.
126. Akhtar, M.N.; Khan, S.A.; Mohamed, M.; Janvekar, A.A. Automated image analysis and improvisations to manage palm oil plantation. *IOP Conf. Ser. Mater. Sci. Eng* **2020**, *1007*, 012082. [CrossRef]
127. Zhao, W.; Xu, M.; Cheng, X.; Zhao, Z. An Insulator in Transmission Lines Recognition and Fault Detection Model Based on Improved Faster RCNN. *IEEE Trans. Instrum. Meas.* **2021**, *70*, 5016408. [CrossRef]
128. Ai, S.; Li, C.; Li, X.; Jiang, T.; Grzegorzek, M.; Sun, C.; Rahaman, M.; Zhang, J.; Yao, Y.; Li, H. A State-of-the-Art Review for Gastric Histopathology Image Analysis Approaches and Future Development. *BioMed Res. Int.* **2021**, *2021*, 6671417. [CrossRef]
129. Singh, A.; Pannu, H.S.; Malhi, A. Explainable information retrieval using deep learning for medical images. *Comput. Sci. Inf. Syst.* **2022**, *19*, 277–307. [CrossRef]
130. Hassan, M.A.; Yang, M.; Rasheed, A.; Yang, G.; Reynolds, M.; Xia, X.; Xiao, Y.; He, Z. A rapid monitoring of NDVI across the wheat growth cycle for grain yield prediction using a multi-spectral UAV platform. *Plant Sci.* **2018**, *282*, 95–103. [CrossRef]
131. Wahab, I.; Hall, O.; Jirström, M. Remote Sensing of Yields: Application of UAV Imagery-Derived NDVI for Estimating Maize Vigor and Yields in Complex Farming Systems in Sub-Saharan Africa. *Drones* **2018**, *2*, 28. [CrossRef]
132. Khan, N.; Kamaruddin, M.A.; Sheikh, U.U.; Yusup, Y.; Bakht, M.P. Oil Palm and Machine Learning: Reviewing One Decade of Ideas, Innovations, Applications, and Gaps. *Agriculture* **2021**, *11*, 832. [CrossRef]
133. da Silva, M.J.; Magalhães, P.S.G. Modeling and design of an injection dosing system for site-specific management using liquid fertilizer. *Precis. Agric.* **2018**, *20*, 649–662. [CrossRef]
134. Xin, F.; Zhao, J.; Zhou, Y.; Wang, G.; Han, X.; Fu, W.; Lan, Y. Effects of Dosage and Spraying Volume on Cotton Defo-liants Efficacy: A Case Study Based on Application of Unmanned Aerial Vehicles. *Agronomy* **2018**, *8*, 85. [CrossRef]
135. Lakshmi, J.; Naresh, G. A Review on Developing Tech-Agriculture using Deep Learning Methods by Applying UAVs. *Int. J. Sci. Res. Comput. Sci. Eng. Inf. Technol.* **2018**, *3*, 1858–1863.
136. Zhang, Y.; Chen, D.; Wang, S.; Tian, L. A promising trend for field information collection: An air-ground multi-sensor monitoring system. *Inf. Process. Agric.* **2018**, *5*, 224–233. [CrossRef]
137. Van Loon, J.; Speratti, A.B.; Gabarra, L.; Govaerts, B. Precision for Smallholder Farmers: A Small-Scale-Tailored Variable Rate Fertilizer Application Kit. *Agriculture* **2018**, *8*, 48. [CrossRef]
138. Ansari, E.; Akhtar, M.N.; Abdullah, M.N.; Othman, W.A.; Bakar, E.A.; Hawary, A.F.; Alhady, S.S. Image Processing of UAV Imagery for River Feature Recognition of Kerian River, Malaysia. *Sustainability* **2021**, *13*, 9568. [CrossRef]